A Hyperbolic Theory for Advection-Diffusion Problems: Mathematical Foundations and Numerical Modeling

**Hector Gomez · Ignasi Colominas · Fermín Navarrina ·
José París · Manuel Casteleiro**

Abstract Linear parabolic diffusion theories based on Fourier's or Fick's laws predict that disturbances can propagate at infinite speed. Although in some applications, the infinite speed paradox may be ignored, there are many other applications in which a theory that predicts propagation at finite speed is mandatory. As a consequence, several alternatives to the linear parabolic diffusion theory, that aim at avoiding the infinite speed paradox, have been proposed over the years. This paper is devoted to the mathematical, physical and numerical analysis of a hyperbolic convection-diffusion theory.

1 Introduction

There is overwhelming experimental evidence showing that diffusive processes take place with finite velocity inside matter [25, 69, 71]. From a theoretical standpoint, it is even clearer that mass and energy cannot propagate at infinite speed. However, linear parabolic diffusion theories based on Fick's law [33] or Fourier's laws [35] (in the case of mass transport or heat conduction, respectively) predict an infinite speed of propagation. It is true that although the linear parabolic theory propagates disturbances at an infinite speed, their amplitudes decay exponentially. For this reason, in some applications, this issue can be ignored and the use of linear parabolic models may be accurate enough for practical purposes in spite of predicting an infinite speed of propagation [16]. However, in many other applications it is necessary to take into account the wave nature of diffusive processes to perform accurate predictions [25, 76, 82]. As a consequence, several alternatives to the linear parabolic diffusion theory, that aim at avoiding the infinite speed paradox, have been proposed over the years. Although there are other possibilities most of the proposed models pertain either to the hyperbolic diffusion theory or the nonlinear parabolic theory. In this paper we analyze in detail a hyperbolic convection-diffusion theory that has been recently proposed by the authors [42–44].

The hyperbolic diffusion theory was initiated in 1958 by Cattaneo who proposed a generalization of Fourier's and Fick's law that overcomes the infinite speed paradox. Cattaneo's work had an enormous impact and his theory is still the most widely accepted generalization of the linear parabolic theory. However, there is also some criticism to Cattaneo's law [1, 32, 47, 55, 56]. Over the years, Cattaneo's equation has been derived using different arguments. Maxwell [67], Cattaneo [15] and Grad [46] obtained the equation using the kinetic theory. Goldstein [37] derived Cattaneo's equation from a correlated random walk using a limiting process. Tavernier [78], on the other hand, departed from Boltzmann's equation. Finally, Kaliski [62] derived the hyperbolic diffusion equation assuming finite propagation velocity as an axiom.

The study of hyperbolic diffusion has been mainly limited to pure-diffusive problems heretofore [57, 58, 74, 89]. The authors have recently proposed a generalization of the hyperbolic diffusion equation that can also be used in convective cases [38–40]. From a numerical point of view, the simulation of the hyperbolic diffusion equation has been mostly limited to 1D problems [3, 12]. The numerical discretization of 2D pure-diffusion problems was probably pioneered by Yang [88]. Later, Manzari et al. [66] proposed a different algorithm and solved some practical pure-diffusive

H. Gomez · I. Colominas (✉) · F. Navarrina · J. París ·
M. Casteleiro
Department of Mathematical Methods, Civil Engineering School,
A Coruña, Spain
e-mail: icolominas@udc.es

examples. In [48] the authors proposed a hybrid technique based on the Laplace transform and finite volume methods. Hoashi et al. developed in [50] a numerical method based on the cubic interpolated method [87]. More recently, several techniques based on the discontinuous Galerkin method have been proposed [43, 86].

In this paper we present two numerical formulations for the hyperbolic convection-diffusion theory. We solve several numerical examples that illustrate the main characteristics of the hyperbolic theory and the robustness of our numerical formulation.

The outline of this paper is as follows: In Sect. 2 we review three theories for pure diffusion. Section 3 presents and analyzes our hyperbolic theory for convection-diffusion. In Sect. 4 we develop a numerical analysis of the one-dimensional stationary hyperbolic convection-diffusion theory. In Sect. 5 we present a finite element formulation for the hyperbolic convection-diffusion theory and solve some numerical examples that illustrate the main characteristics of our theory. In Sect. 6 we introduce a discontinuous Galerkin method for the hyperbolic theory. We test out this formulation with several examples focusing on the accuracy of the formulation for smooth solutions and its robustness for convection-dominated problems.

2 Mathematical Models for Pure-Diffusive Problems

In this section we present and analyze three theories for pure diffusion: the linear parabolic model, the nonlinear parabolic theory and the hyperbolic model. Although most of what we present in this paper is valid for heat and mass diffusion we use the terminology of mass transfer. Therefore, when we say pure diffusion (or simply diffusion) we mean the diffusion of a pollutant within a static fluid. We call convection-diffusion to the diffusion of a pollutant within an incompressible flow which may move with respect to our reference.

2.1 Classical Linear Parabolic Diffusion Theory

The classical theory for pure-diffusive processes is defined by the equations:

$$\frac{\partial u}{\partial t} + \nabla \cdot \boldsymbol{q} = f, \tag{1.1}$$

$$\boldsymbol{q} = -\boldsymbol{K}\nabla u. \tag{1.2}$$

In the context of mass diffusion, u represents the pollutant concentration, $\boldsymbol{q}$ is the pollutant flux, f is a source term and $\boldsymbol{K}$ is the diffusivity tensor which is assumed positive definite and independent of u. Equation (1.1) is the mass conservation equation and (1.2) the constitutive equation that defines

the pollutant flux. We observe that system (1) is equivalent to the scalar equation

$$\frac{\partial u}{\partial t} - \nabla \cdot (\boldsymbol{K}\nabla u) = f. \tag{2}$$

Let us consider the Cauchy problem given by equation (2) and suitable initial conditions, namely: find $u : \mathbb{R}^3 \times [0, T] \mapsto \mathbb{R}$ such that,

$$\frac{\partial u}{\partial t} - \nabla \cdot (\boldsymbol{K}\nabla u) = f \quad \text{in } \mathbb{R}^3 \times (0, T), \tag{3.1}$$

$$u(\boldsymbol{x}, 0) = u_0(\boldsymbol{x}) \quad \text{in } \mathbb{R}^3. \tag{3.2}$$

It is a known fact that the Cauchy problem (3) describes a process were disturbances propagate at infinite speed. We say that disturbances move at an infinite speed if for a compactly supported initial condition $u_0(\boldsymbol{x})$, the solution to the Cauchy problem (3) at a given time t is not compactly supported as a function of $\boldsymbol{x}$. We illustrate this fact with a one-dimensional example. Let us consider an homogeneous and isotropic medium (hence, if $\boldsymbol{I}$ is the identity tensor, $\boldsymbol{K} = k\boldsymbol{I}$ for a certain $k > 0$). We do not consider source terms. We analyze the following Cauchy problem: find $u : \mathbb{R} \times \mathbb{R}^+ \mapsto \mathbb{R}$ such that

$$\frac{\partial u}{\partial t} - k\frac{\partial^2 u}{\partial x^2} = 0 \quad \forall x \in \mathbb{R}, \ t > 0. \tag{4.1}$$

$$u(x, 0) = \delta(x) \quad \forall x \in \mathbb{R}. \tag{4.2}$$

where δ is the Dirac distribution. The exact solution of (4) is

$$u(x, t) = \frac{1}{\sqrt{4\pi kt}}e^{-\frac{x^2}{4kt}} \quad \forall x \in \mathbb{R}, \ t > 0. \tag{5}$$

Therefore, for any time $t > 0$, the pollutant concentration is given by the Gauss distribution function, which is not a compactly supported function of x, as we had anticipated. Figure 1 shows (in dashed line) the solution of (4) for $k = 1$ at $t = 4$ and $t = 10$.

Remark 1 It may be argued that in practical applications the infinite speed paradox is not very relevant because, although disturbances propagate at an infinite speed, their amplitudes decay exponentially with distance. We believe that in some applications the infinite speed paradox can be ignored and the use of parabolic models may be accurate enough for practical purposes in spite of predicting non-physical velocities of propagation. However, in many other applications it is necessary to take into account the wave nature of diffusive processes to perform accurate predictions [25, 82]. Therefore, an alternative to the linear parabolic model is desirable.
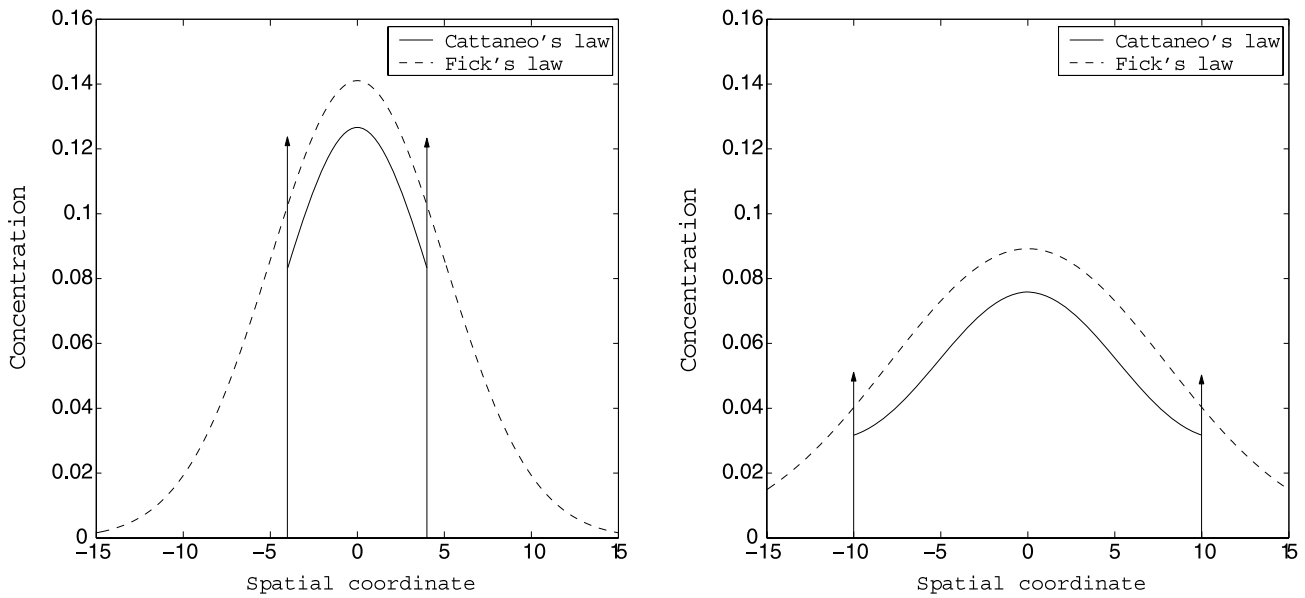
Fig. 1 Comparison at $t = 4$ (*left*) and at $t = 10$ (*right*) between the solution of (4) (*dashed line*) and the solution of (13) (*solid line*). *The vertical arrows* represent Dirac's distributions. Parameters k and τ have a value of one

2.2 Nonlinear Parabolic Diffusion Theory

Although the main objective of this paper is the study of the linear hyperbolic diffusion theory, we would like at least to mention the nonlinear parabolic diffusion theory, which in some instances leads to finite velocity of propagation. The distinctive feature of the nonlinear parabolic diffusion theory is that the diffusivity depends on the concentration or its spatial derivatives. Mathematically, we represent this fact using the notation $\boldsymbol{K}(u, \nabla u)$. For simplicity, we will restrict ourselves to isotropic media and so, $\boldsymbol{K}(u, \nabla u) = k(u, \nabla u)\boldsymbol{I}$, where $k(u, \nabla u) \geq 0$.

The first nonlinear parabolic diffusion theory was introduced in 1950 by Zel'dovich and Kompaneets [90]. In this paper, the authors focus on plasma radiation at high temperatures and they argue that the diffusivity depends on the temperature through a power law. After this publication, the interest on the topic grew enormously, especially in the mathematics community.

Zel'dovich and Kompaneets solved in [90] the following Cauchy problem: find $u : \mathbb{R}^3 \times [0, T] \mapsto \mathbb{R}$ such that

$$\frac{\partial u}{\partial t} - \nabla \cdot \left(k(u, \nabla u) \nabla u \right) = 0 \quad \text{in } \mathbb{R}^3 \times (0, T) \qquad (6.1)$$

$$u(\boldsymbol{x}, 0) = u_0(\boldsymbol{x}) \quad \text{on } \mathbb{R}^3 \qquad (6.2)$$

where

$$k(u, \nabla u) = u^m, \quad m > 0. \qquad (7)$$

Under the assumption of spherical symmetry, they obtained the solution to (6) and proved that it is a compactly supported function of $\boldsymbol{x}$ for all t [7, 68]. Thus, we say that this

equation leads to finite velocity of propagation. The solution to (6) was also obtained by Barenblatt [5] in the context of ground water filtration and by Pattle [70]. For a review of this type of equations we refer the reader to the fundamental review by Kalashnikov [60] or the books by Vázquez [81] and Antontsev et al. [2] that cover in great detail the mathematics of this equation. We also recommend the read of the books by Landau and Lifshitz [64] (see Chap. 16) and Kalatnikov [61].

Remark 2 Equation (6.1) with $k(u, \nabla u) = u^m$, $m > 0$ pertains to the so-called degenerate parabolic equations. Wherever $u = 0$, the equation becomes hyperbolic. This fact gives rise to the finite velocity of propagation. From a physical standpoint, it may be argued that this is not very relevant in a heat conduction problem because temperature will never vanish.

Remark 3 Although the finite velocity of propagation for parabolic problems is an intrinsically nonlinear phenomenon, not every function k leads to finite velocity of propagation. Another typical example of nonlinear parabolic equation with finite speed of propagation is given by the diffusivity

$$k(u, \nabla u) = |\nabla u|^p; \ p > 0 \qquad (8)$$

which defines the so-called p-Laplacian equation.

2.3 Hyperbolic Diffusion Theory

The hyperbolic diffusion theory is derived substituting in system (1) Fick's law by a more general equation due to

Cattaneo [16], namely

$$q + \tau \frac{\partial q}{\partial t} = -K \nabla u. \tag{9}$$

In equation (9), τ is the so-called relaxation tensor which has dimensions of time. Then, the hyperbolic diffusion theory is defined by the following set of equations:

$$\frac{\partial u}{\partial t} + \nabla \cdot q = f, \tag{10.1}$$

$$q + \tau \frac{\partial q}{\partial t} = -K \nabla u. \tag{10.2}$$

We observe that when $\tau = 0$ we retrieve the parabolic theory. Also, at the steady state, both theories are equivalent even for $\tau \neq 0$. Under certain assumptions, the pollutant flux can be eliminated in system (10). Let us assume isotropic and homogeneous medium. Then, $K = kI$, $\tau = \tau I$ for certain $k > 0$, $\tau > 0$. We do not consider source terms. After eliminating the pollutant flux in system (10), we obtain the so-called hyperbolic diffusion equation,

$$\tau \frac{\partial^2 u}{\partial t^2} + \frac{\partial u}{\partial t} - k \Delta u = 0. \tag{11}$$

Equation (11) is hyperbolic and, as a consequence, we can define a finite velocity for the pollutant transport, namely

$$c = \sqrt{k/\tau}. \tag{12}$$

To compare the solution of the classic formulation with the solution of the hyperbolic theory we solve the hyperbolic counterpart of (4). Now, we need two initial conditions because (11) involves second-order derivatives with respect to time. We consider a homogeneous, isotropic and one-dimensional medium. With the above hypotheses we can state the problem as: find $u \colon \mathbb{R} \times \mathbb{R}^+ \mapsto \mathbb{R}$ such that

$$\tau \frac{\partial^2 u}{\partial t^2} + \frac{\partial u}{\partial t} - k \frac{\partial^2 u}{\partial x^2} = 0 \quad \forall x \in \mathbb{R}, \ t > 0, \tag{13.1}$$

$$u(x, 0) = \delta(x) \quad \forall x \in \mathbb{R}, \tag{13.2}$$

$$\frac{\partial u}{\partial t}(x, 0) = 0 \quad \forall x \in \mathbb{R}. \tag{13.3}$$

We may solve (13) using Fourier and Laplace transforms in space and time, respectively (see reference [38] for a detailed resolution). The solution to (13) may be written as,

$$u(x, t) = \begin{cases} \frac{1}{2} e^{-\frac{c^2}{2k}t} \left[\delta(|x| - ct) + \frac{c}{2k} I_0\left(\frac{c}{2k}\sqrt{c^2 t^2 - x^2}\right) \right. \\ \left. + \frac{c^2}{2k} t \frac{I_1\left(\frac{c}{2k}\sqrt{c^2 t^2 - x^2}\right)}{\sqrt{c^2 t^2 - x^2}} \right], \quad |x| \leq ct \\ 0, \quad |x| > ct \end{cases} \tag{14}$$

where I_0 and I_1 are the modified Bessel functions of the first kind of order 0 and 1. Equation (14) clearly illustrates

that the hyperbolic diffusion theory predicts the existence of a wave front that advances with velocity c. In Figure 1 we compare the solutions to (4) and (13) at $t = 4$ and $t = 10$, respectively.

Remark 4 There are several experiments showing the existence of heat waves in liquid helium and dielectric crystals. Apparently, Peshkov [71] was the first to measure experimentally the velocity of heat waves.

Remark 5 Although Cattaneo's law was proposed as a generalization of Fourier's law, the scientific community agrees that it may be also thought of as a generalization of Fick's law. Actually, Cattaneo's law is considered to have potential in representing anomalous mass transport phenomena [25], which has become extremely important in the last decade [63].

Remark 6 A common criticism to Cattaneo's law is that in most applications the relaxation time is very small. Given that Cattaneo's and Fick's laws are equivalent at the steady state, we would only see differences at the shortest time scales. We believe that this may be true in some applications, but we also remark that in the realm of heat conduction there are systems characterized by long relaxation times. Prime examples are polymeric fluids, heat and electric conductors at high temperatures or superconductors. Moreover, for the case of mass transfer, the relaxation time is believed to be several orders of magnitude larger than in heat propagation problems.

Remark 7 Cattaneo's law may be derived as a particular case of the theory proposed by Gurtin and Pipkin [45]. According to this theory, the pollutant flux at a given time may be expressed as an integral over the history of the concentration gradient. In particular,

$$q(x, t) = -\int_{-\infty}^{t} \psi(t - s) \nabla u(x, s) \mathrm{d}s \tag{15}$$

where $\psi(z)$ is a positive, decreasing kernel that tends to zero as z tends to infinity. Cattaneo's law for isotropic media is retrieved for $\psi(z) = \frac{k}{\tau} e^{-z/\tau}$.

Remark 8 Wilhelm and Choi [85] proposed an interesting generalization of the theories presented in Sects. 2.2 and 2.3. The authors used Cattaneo's law with a concentration-dependent diffusivity and relaxation time. Reverberi et al. [73] have recently presented numerical results using Cattaneo's law with concentration-dependent diffusivity.

2.3.1 Dispersion Relation

In this section we show that the hyperbolic diffusion theory exhibits a dispersive behavior [3]. For the sake of simplicity,

we restrict ourselves to the one-dimensional, homogeneous and isotropic setting. Let us consider a solution of the type

$$\begin{pmatrix} u \\ q \end{pmatrix} = \begin{pmatrix} \mathcal{U} \\ \mathcal{Q} \end{pmatrix} e^{i(\omega t - \xi x)} \tag{16}$$

where $i^2 = -1$. The previous ansatz leads to the dispersion relation

$$\omega i = \tau \omega^2 - k \xi^2. \tag{17}$$

For an initial value problem, ξ is a real wave number and ω a complex frequency. Let us rewrite ω as

$$\omega = \omega_R + i \omega_C \tag{18}$$

where ω_R is a real frequency and ω_C is a damping coefficient. Introducing (18) in the dispersion relation (17), we obtain

$$\frac{\omega_R}{\xi} = \begin{cases} 0, & \xi \leq \frac{1}{2\tau c} \\ \pm\sqrt{c^2 - \frac{1}{4\tau^2 \xi^2}}, & \xi > \frac{1}{2\tau c} \end{cases} \tag{19.1}$$

$$\omega_C = \begin{cases} \frac{1}{2\tau}(1 \pm \sqrt{1 - 4\tau^2 c^2 \xi^2}), & \xi < \frac{1}{2\tau c} \\ \frac{1}{2\tau}, & \xi \geq \frac{1}{2\tau c} \end{cases} \tag{19.2}$$

where ω_R/ξ is the wave velocity and ω_C is the damping coefficient. Equations (19) show that a Fourier mode defined by the wave number ξ travels with velocity $\omega_R(\xi)/\xi$ and is damped at a rate $e^{-\omega_C(\xi)t}$. In Figs. 2 and 3 we represent, respectively, the wave velocity and the damping rate $e^{-\omega_C t}$ versus the wave number ξ, assuming $k = \tau = t = 1$. We observe that there is a bifurcation point at the wave number $\xi = \frac{1}{2\tau c}$. The asymptotic wave velocity as the wave number tends to infinity is $\sqrt{k/\tau}$. The damping ratio is $e^{-1/(2\tau)}$ for all modes with wave numbers within the interval $[1/(2\tau c), \infty)$.

Remark 9 From a physical standpoint, the dispersive character of the equations adequately represents the physics of the problem. For example, in the context of heat conduction the wave velocity depends on the amount of energy transported by the heat wave [57, 58].

2.3.2 Thermodynamics

While the parabolic diffusion theory fits nicely within the framework of Classical Irreversible Thermodynamics, the hyperbolic theory is incompatible with it. The reason for that is the hyperbolic diffusion theory leads to negative entropy production in some circumstances. Let us call σ the entropy
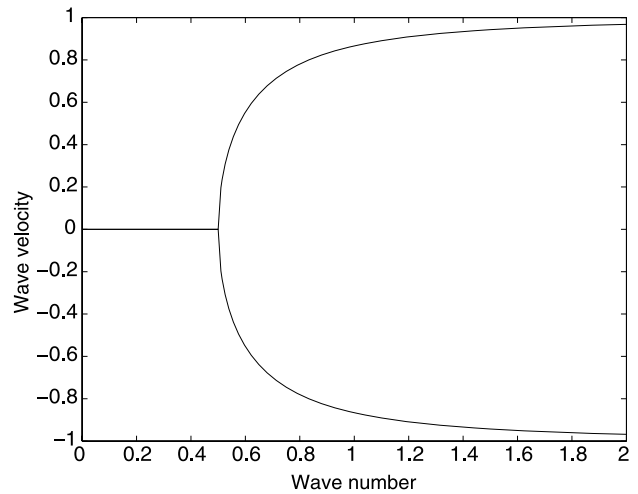

Fig. 2 Wave velocity $\omega_R(\xi)/\xi$ for a Fourier mode defined by the wave number ξ
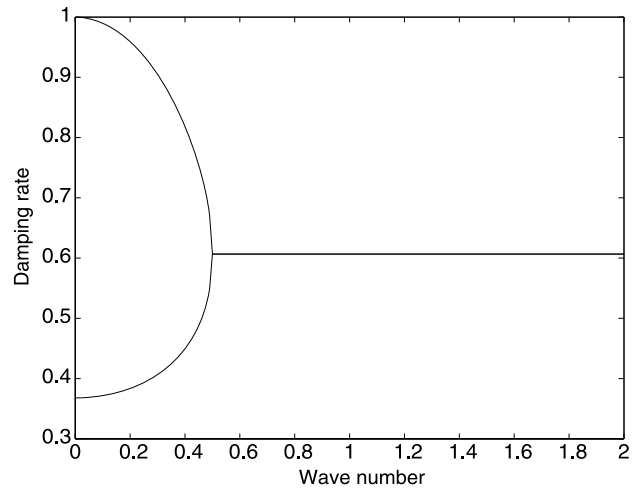

Fig. 3 Damping rate $e^{-\omega_C(\xi)t}$ for a Fourier mode defined by the wave number ξ

production. According to Classical Irreversible Thermodynamics,

$$\sigma = \boldsymbol{q} \cdot \nabla \left(\frac{1}{u}\right). \tag{20}$$

Applying this expression to the hyperbolic diffusion theory, we get

$$\sigma = \frac{k}{u^2} \|\nabla u\|^2 + \frac{\tau}{u^2} \frac{\partial \boldsymbol{q}}{\partial t} \cdot \nabla u \tag{21}$$

where $\|\cdot\|$ denotes the Euclidean norm of a given vector. The entropy production in (21) is not always positive when $\tau \neq 0$. It is commonly accepted [59] that this fact is due to the hypothesis of local equilibrium that underlies Classical Irreversible Thermodynamics. This is one of the reasons why the physics community is trying to extend the

thermodynamics theory to non-equilibrium systems. The so-called Extended Irreversible Thermodynamics seems to be a promising candidate. The central quantity of this theory is a generalized non-equilibrium entropy that depends not only on the classical variables, but also on the dissipative fluxes. The hyperbolic diffusion theory is compatible with Extended Irreversible Thermodynamics.

3 Hyperbolic Convection-Diffusion Theory

In the context of many engineering applications of mass transport, such as the evolution of a pollutant spilled in a port, it is important to consider not only the diffusion mechanism but also the transport due to convection. For this reason, it is of prime importance to extend the diffusion theories to convective situations. We suppose that convection is driven by the movement of a fluid that we assume incompressible throughout the paper.

The parabolic model can be easily extended to convective problems, just by adding the standard convective term to the equations. The extension of the hyperbolic model to moving domains is not straightforward and has been improperly used in the literature several times. Unlike Fick's law, Cattaneo's law has to be modified in the presence of convection. Otherwise, the resulting model is not invariant under Galilean transformations. The authors proposed [38, 40, 42] (see also [17]) a generalized version of Cattaneo's law that may be used in convective problems, namely

$$q + \tau \left(\frac{\partial q}{\partial t} + \nabla q \, a \right) = -K \nabla u. \tag{22}$$

Thus, the governing equations for our hyperbolic convection-diffusion theory are given by:

$$\frac{\partial u}{\partial t} + a \cdot \nabla u + \nabla \cdot q = 0, \tag{23.1}$$

$$q + \tau \left(\frac{\partial q}{\partial t} + \nabla q \, a \right) = -K \nabla u. \tag{23.2}$$

A remarkable fact is that the hyperbolic convection-diffusion theory is *not* equivalent to the parabolic convection-diffusion theory at the steady state. This entails that for a non-zero relaxation time, both theories would predict different results *at all time scales*.

3.1 The Effect of Convection on the Hyperbolic Diffusion Theory

Simple arguments from dimensional analysis show that the effect of convection is much stronger on the hyperbolic theory than on the linear parabolic model. We will illustrate

this fact with a one-dimensional example in which we assume that there are no sources and the medium is homogeneous and isotropic. Under these conditions, in the parabolic model, space and time can always be rescaled to keep the solution invariant with respect to changes in the parameters (here velocity is considered a parameter) both in pure-diffusive and in convective-diffusive problems. In the hyperbolic theory that is true only in absence of convection. To show this, we consider equations (23) under the above mentioned hypotheses, that is,

$$\frac{\partial u}{\partial t} + a \frac{\partial u}{\partial x} + \frac{\partial q}{\partial x} = 0, \tag{24.1}$$

$$q + \tau \frac{\partial q}{\partial t} + \tau a \frac{\partial q}{\partial x} = -k \frac{\partial u}{\partial x}. \tag{24.2}$$

All the physical quantities involved in (24) can be measured using units of measurement that belong to the LT class, in which units of length and time are chosen as fundamental units. Due to the fundamental principle which states that physical laws do not depend on arbitrarily chosen units of measurement [6], we can rescale length and time by arbitrary positive numbers. Let us rescale the units of measurement of time by τ and length by $a\tau$. Let us denote by $\hat{\phi}$ the value of the physical quantity ϕ in the new system of units. Thus, the equations in the new system of units read as:

$$\frac{\partial \hat{u}}{\partial \hat{t}} + \frac{\partial \hat{u}}{\partial \hat{x}} + \frac{\partial \hat{q}}{\partial \hat{x}} = 0, \tag{25.1}$$

$$\hat{q} + \frac{\partial \hat{q}}{\partial \hat{t}} + \frac{\partial \hat{q}}{\partial \hat{x}} = -H^{-2} \frac{\partial \hat{u}}{\partial \hat{x}}, \tag{25.2}$$

where

$$H = a/c. \tag{26}$$

Equations (25)–(26) clearly show that space and time no longer can be rescaled to keep the solution invariant with respect to changes in the parameters. The solution of the hyperbolic convection-diffusion theory intrinsically depends on H, a dimensionless number which plays a similar role to Mach number in compressible flow. This will be studied in detail in the next section.

3.2 Conservation Form of the Hyperbolic Convection-Diffusion Theory

The authors proposed in [42] a conservation form for system (23). Under the assumptions of homogeneity, isotropy and incompressibility of the fluid, the governing equations of the hyperbolic convection-diffusion theory may be written as

$$\frac{\partial u}{\partial t} + \nabla \cdot (ua + q) = 0, \tag{27.1}$$

$$\frac{\partial(\tau \boldsymbol{q})}{\partial t} + \nabla \cdot (\tau \boldsymbol{q} \otimes \boldsymbol{a} + ku\boldsymbol{I}) + \boldsymbol{q} = 0. \tag{27.2}$$

System (27) can also be written in compact form as:

$$\frac{\partial \boldsymbol{U}}{\partial t} + \nabla \cdot \boldsymbol{F} = \boldsymbol{S} \tag{28}$$

where

$$\boldsymbol{U} = \begin{pmatrix} u \\ \tau q_1 \\ \tau q_2 \\ \tau q_3 \end{pmatrix};$$

$$\boldsymbol{F} = \begin{pmatrix} ua_1 + q_1 & ua_2 + q_2 & ua_3 + q_3 \\ \tau q_1 a_1 + ku & \tau q_1 a_2 & \tau q_1 a_3 \\ \tau q_2 a_1 & \tau q_2 a_2 + ku & \tau q_2 a_3 \\ \tau q_3 a_1 & \tau q_3 a_2 & \tau q_3 a_3 + ku \end{pmatrix}; \tag{29}$$

$$\boldsymbol{S} = \begin{pmatrix} 0 \\ -q_1 \\ -q_2 \\ -q_3 \end{pmatrix}$$

and q_i, a_i denote, respectively, the Cartesian components of $\boldsymbol{q}$ and $\boldsymbol{a}$. To study the basic properties of equation (28) it is convenient to rewrite it in non-conservative form. If we define $\boldsymbol{F}_i$ as the i-th column of matrix $\boldsymbol{F}$, the following relation holds:

$$\nabla \cdot \boldsymbol{F} = \frac{\partial \boldsymbol{F}_i}{\partial x_i} = \boldsymbol{A}_i \frac{\partial \boldsymbol{U}}{\partial x_i}, \quad i = 1, 2, 3, \tag{30}$$

where repeated indices indicate summation (we will use this convention throughout this section) and

$$\boldsymbol{A}_i = \frac{\partial \boldsymbol{F}_i}{\partial \boldsymbol{U}} \tag{31}$$

are the Jacobian matrices whose component-wise representation is

$$\boldsymbol{A}_1 = \begin{pmatrix} a_1 & 1/\tau & 0 & 0 \\ k & a_1 & 0 & 0 \\ 0 & 0 & a_1 & 0 \\ 0 & 0 & 0 & a_1 \end{pmatrix};$$

$$\boldsymbol{A}_2 = \begin{pmatrix} a_2 & 0 & 1/\tau & 0 \\ 0 & a_2 & 0 & 0 \\ k & 0 & a_2 & 0 \\ 0 & 0 & 0 & a_2 \end{pmatrix}; \tag{32}$$

$$\boldsymbol{A}_3 = \begin{pmatrix} a_3 & 0 & 0 & 1/\tau \\ 0 & a_3 & 0 & 0 \\ 0 & 0 & a_3 & 0 \\ k & 0 & 0 & a_3 \end{pmatrix}.$$

Let us define $\boldsymbol{\kappa} \in \mathbb{R}^3$, $\|\boldsymbol{\kappa}\| = 1$, otherwise arbitrary. System (28) is totally hyperbolic if the equation

$$\det(\omega_{\boldsymbol{\kappa}} \boldsymbol{I} - \boldsymbol{A}_i \kappa_i) = 0 \tag{33}$$

yields four different real solutions $\omega_{\boldsymbol{\kappa}}$ for arbitrarily prescribed values of $\boldsymbol{\kappa}$ [26]. It is easy to prove that the solutions to (33) are

$$\omega_{\boldsymbol{\kappa}}^1 = \boldsymbol{a} \cdot \boldsymbol{\kappa}, \tag{34.1}$$

$$\omega_{\boldsymbol{\kappa}}^2 = \boldsymbol{a} \cdot \boldsymbol{\kappa}, \tag{34.2}$$

$$\omega_{\boldsymbol{\kappa}}^3 = \boldsymbol{a} \cdot \boldsymbol{\kappa} - c, \tag{34.3}$$

$$\omega_{\boldsymbol{\kappa}}^4 = \boldsymbol{a} \cdot \boldsymbol{\kappa} + c, \tag{34.4}$$

which are all real numbers. Therefore, system (28) is hyperbolic. The $\omega_{\boldsymbol{\kappa}}^i$'s in (34) are the eigenvalues of $\boldsymbol{A}_i \kappa_i$ which is usually referred to as *projection matrix*. Now, by making some basic algebraic work we can compute the eigenvectors of $\boldsymbol{A}_i \kappa_i$. Then, we can define the square matrix $\boldsymbol{C}_{\boldsymbol{\kappa}}$ as the matrix whose columns are the eigenvectors of the projection matrix, that is,

$$\boldsymbol{C}_{\boldsymbol{\kappa}} = \begin{pmatrix} 0 & 0 & c & c \\ -\kappa_3 & -\kappa_2 & -k\kappa_1 & k\kappa_1 \\ 0 & \kappa_1 & -k\kappa_2 & k\kappa_2 \\ \kappa_1 & 0 & -k\kappa_3 & k\kappa_3 \end{pmatrix}. \tag{35}$$

Let $\boldsymbol{\Lambda}_{\boldsymbol{\kappa}}$ be the diagonal matrix such that the elements placed in the main diagonal are the eigenvalues $\omega_{\boldsymbol{\kappa}}^i$, $i = 1, \ldots, 4$. Then, the following relation holds

$$\boldsymbol{\Lambda}_{\boldsymbol{\kappa}} = \boldsymbol{C}_{\boldsymbol{\kappa}}^{-1} \boldsymbol{A}_i \kappa_i \boldsymbol{C}_{\boldsymbol{\kappa}}. \tag{36}$$

At this point, we define the following dimensionless number

$$H = \frac{\|\boldsymbol{a}\|}{c} \tag{37}$$

which plays a similar role to Mach number in compressible flow problems [27] or to the Froude number in shallow water problems [84]. By using this dimensionless number we can define three types of flow

- $H < 1 \Leftrightarrow$ Subcritical flow
- $H > 1 \Leftrightarrow$ Supercritical flow
- $H = 1 \Leftrightarrow$ Critical flow

Observe that upstream pollutant transport is not possible in supercritical flow conditions, since the velocity of the diffusive mode of propagation is smaller than the velocity of the convective mode.

3.3 Boundary Conditions

In [41] we proved that, for one-dimensional problems, it is possible to diagonalize the hyperbolic system (28) and

define the Riemann variables (see [51] for an introduction to hyperbolic systems). Unfortunately, in three-dimensional problems, matrices A_i are not diagonalizable in the same basis, which makes impossible to diagonalize system (28). However, given a direction κ, it is possible to define the characteristic variables, which are the analogue of Riemann variables for the direction κ. To impose boundary conditions, we need to define the characteristic variables in the outward normal direction to the boundary of the computational domain. Let us call n a vector pointing in that direction and verifying $\|n\| = 1$. For our hyperbolic convection-diffusion theory the characteristic variables are defined as,

$$Y^n = C_n^{-1} U \tag{38}$$

where matrix C_n^{-1} may be obtained from equation (35). If we call Y_i^n, $i = 1, \ldots, 4$ the components of Y^n, then

$$Y_1^n = \tau \left(-n_3 q_1 - \frac{n_2 n_3}{n_1} q_2 + \frac{n_1^2 + n_2^2}{n_1} q_3 \right), \tag{39.1}$$

$$Y_2^n = \tau \left(-n_2 q_1 + \frac{n_1^2 + n_3^2}{n_1} q_2 - \frac{n_2 n_3}{n_1} q_3 \right), \tag{39.2}$$

$$Y_3^n = \frac{1}{2c} \left(u - \frac{1}{c} q \cdot n \right), \tag{39.3}$$

$$Y_4^n = \frac{1}{2c} \left(u + \frac{1}{c} q \cdot n \right). \tag{39.4}$$

At a given point of the boundary we need to impose Y_i^n if and only if ω_n^i is negative, where the ω_n^i are the eigenvalues in the direction n which may be obtained from (34).
Let us define H_n as

$$H_n = \frac{a \cdot n}{c} \tag{40}$$

which is the analogue of the H number for a given direction n. We call inflow boundary the subset of the boundary where $a \cdot n < 0$ and outflow boundary the subset where $a \cdot n > 0$. We say that the flow is subcritical at a given point of the boundary if and only if $H_n < 1$. Wherever $H_n > 1$ the flow is supercritical. Taking into account all of this, we are ready to define boundary conditions for our theory in any situation. In Table 1 we present a summary of quantities to be imposed on the boundary for a three-dimensional problem.

Assuming homogeneous and isotropic medium, and incompressibility of the fluid, the initial/boundary-value problem for our hyperbolic convection-diffusion theory can be

Table 1 Summary of quantities to be imposed on the boundary for the three-dimensional hyperbolic convection-diffusion theory

	Inflow	Outflow
Subcritical	Y_1^n, Y_2^n, Y_3^n	Y_3^n
Supercritical	$Y_1^n, Y_2^n, Y_3^n, Y_4^n$	None

stated as: Given $k, \tau > 0$, given a divergence-free velocity field a and given adequate initial and boundary conditions, find $U : \Omega \times [0, T] \mapsto \mathbb{R}^4$ such that

$$\frac{\partial U}{\partial t} + \nabla \cdot F = S \quad \text{in } \Omega \times (0, T), \tag{41.1}$$

$$U(x, 0) = U_0(x) \quad \text{in } \Omega, \tag{41.2}$$

$$[Y^n] = [Y^n]_D \quad \text{on } \Gamma \times [0, T] \tag{41.3}$$

where $[Y^n]$ represents the subset of Y^n to be imposed at a given point of the boundary and $[Y^n]_D$ denotes the imposed values.

Remark 10 In one-dimensional problems the Riemann variables are given by

$$R = \begin{bmatrix} \frac{1}{2c}(u + \frac{1}{c}q) \\ \frac{1}{2c}(u - \frac{1}{c}q) \end{bmatrix}. \tag{42}$$

In supercritical flows we need to impose both Riemann variables at the inflow boundary and none at the outflow. In subcritical flow, we need to impose one Riemann variable at the inflow boundary and the other at the outflow. Due to the simple structure of the equations in one-dimensional problems, there are other legitimate possibilities. For example, in supercritical flow we may impose u and q at the inlet and leave free all variables at the outlet. In subcritical flow, we may impose concentration on both the inflow and outflow boundaries. We will make use of these boundary conditions in the next section.

4 Numerical Analysis of the One-Dimensional Stationary Hyperbolic Convection-Diffusion Theory

4.1 The Antidiffusion Introduced by Cattaneo's Law

In this section we show that, under adequate assumptions, Cattaneo's law introduces a negative diffusion with respect to Fick's law. We make use of the governing equations for the steady-state, namely

$$\nabla \cdot F = S. \tag{43}$$

For a one-dimensional problem, the previous equation can be rewritten as

$$\frac{dq}{dx} = -a \frac{du}{dx}, \tag{44.1}$$

$$k \frac{du}{dx} + \tau a \frac{dq}{dx} = -q. \tag{44.2}$$

Using (44.1) and the derivative of (44.2), we derive the following second-order equation:

$$a\frac{\mathrm{d}u}{\mathrm{d}x} - (k - \tau a^2)\frac{\mathrm{d}^2u}{\mathrm{d}x^2} = 0. \tag{45}$$

Equation (45) clearly shows that Cattaneo's law introduces a negative diffusion with respect to Fick's law. It may be argued that this fact represents an important drawback of the hyperbolic model because it complicates the numerical resolution of the equation. This is not true. A discussion on this point will be presented in Sect. 4.4.

Remark 11 Note that the coefficient of the second-order term in (45) verifies

$$k - \tau a^2 = k(1 - H^2). \tag{46}$$

Therefore, (45) can be only thought of as the standard parabolic model with a negative diffusion in subcritical flow. In this case the term $k - \tau a^2$ remains positive. In supercritical flow, (45) still makes sense, but the term $k - \tau a^2$ cannot be thought of as a diffusivity, because it takes a negative value.

Remark 12 Equation (45) is not equivalent to system (43). The hyperbolic theory for convection-diffusion is defined by system (43) and not by (45). However, in the case of subcritical flow and Dirichlet boundary conditions both formulations are equivalent if the solutions are sufficiently smooth.

4.2 The Effect of the Standard Galerkin Discretization on the Classic Parabolic Convection-Diffusion Equation

We analyze the classic parabolic convection-diffusion equation subject to Dirichlet boundary conditions (similar studies may be found in [24]). We use the following model problem: find $u : [0, L] \mapsto \mathbb{R}$ such that

$$a\frac{\mathrm{d}u}{\mathrm{d}x} - k\frac{\mathrm{d}^2u}{\mathrm{d}x^2} = 0; \quad x \in (0, L), \tag{47.1}$$

$$u(0) = u_0, \tag{47.2}$$

$$u(L) = u_L. \tag{47.3}$$

Let $\mathcal{P}$ be a uniform partition of $[0, L]$ defined by the points $\{x_i\}_{i=0,N}$ such that $x_i = (i - 1)h$, with $h = L/(N - 1)$. Let us call

$$P_e = \frac{ah}{2k} \tag{48}$$

the *mesh Péclet number* which expresses the ratio of convective to diffusive transport. If we solve (47) using the standard Galerkin method and linear finite elements (this is equivalent to second-order centered finite differences in this

case) we obtain the following discrete equation at an interior node j:

$$(1 - P_e)u_{j+1} - 2u_j + (1 + P_e)u_{j-1} = 0 \tag{49}$$

In (49) u_j is the finite element approximation of $u(x_j)$ and u_0, u_N are the values given by boundary conditions (47.2)–(47.3). Difference equations (49) can be solved exactly (see, for instance, Ref. [54]). The exact solution of (49), subject to boundary conditions (47.2)–(47.3), is

$$u_j = \frac{1}{1 - (\frac{1+P_e}{1-P_e})^N}$$

$$\times \left\{ u_0\left[\left(\frac{1+P_e}{1-P_e}\right)^j - \left(\frac{1+P_e}{1-P_e}\right)^N\right] \right.$$

$$\left. + u_L\left[1 - \left(\frac{1+P_e}{1-P_e}\right)^j\right] \right\}. \tag{50}$$

From (50) it is apparent that the numerical solution will present an oscillatory behavior when $|P_e| > 1$, even though (49) were solved exactly. On the other hand, the exact solution of (47) is

$$u(x_j) = \frac{1}{1 - e^{\frac{ah}{k}N}}[u_0(e^{\frac{ah}{k}j} - e^{\frac{ah}{k}N})$$

$$+ u_L(1 - e^{\frac{ah}{k}j})]. \tag{51}$$

A comparison between (50) and (51) shows that the approximate solution equals the exact solution if the following relation holds

$$e^{2P_e j} = \left(\frac{1+P_e}{1-P_e}\right)^j \quad \forall j = 0, \dots, N. \tag{52}$$

Relation (52) is only satisfied for $P_e = 0$ (pure-diffusive problem). However, using (52) we find that when the mesh is fine enough ($|P_e| \leq 1$) the approximate solution (50) is, actually, the exact solution of the problem

$$a\frac{\mathrm{d}u}{\mathrm{d}x} - k^\star\frac{\mathrm{d}^2u}{\mathrm{d}x^2} = 0; \quad x \in (0, L), \tag{53.1}$$

$$u(0) = u_0, \tag{53.2}$$

$$u(L) = u_L, \tag{53.3}$$

where

$$k^\star = k\frac{2P_e}{\ln(\frac{1+P_e}{1-P_e})}. \tag{54}$$

In Fig. 4 we represent $k^\star/k$ as a function of $P_e \in (-1, 1)$. We observe that $k^\star \to k$ as $|P_e| \to 0$ and $k^\star \to 0$ as $|P_e| \to 1$.
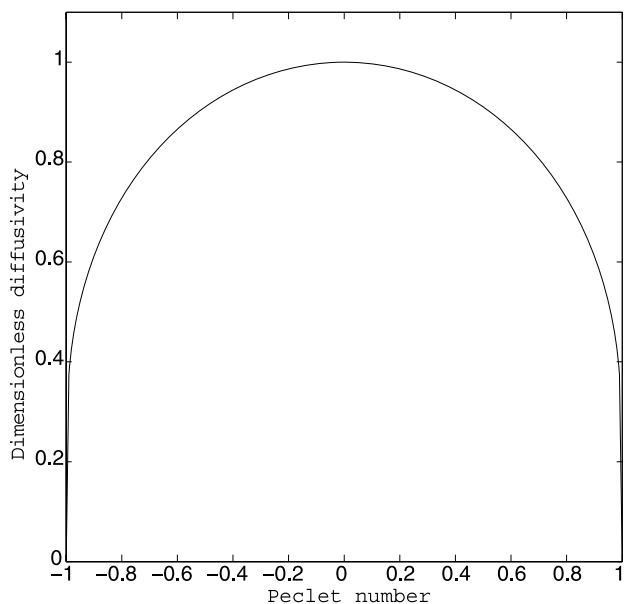
Fig. 4 Dimensionless diffusivity ($k^\star/k$) as a function of $P_\mathrm{e} \in (-1, 1)$

Fig. 5 Dimensionless H number as a function of $P_\mathrm{e} \in (-1, 1)$

Remark 13 If the mesh is fine enough ($|P_\mathrm{e}| < 1$), then $k^\star \in (0, k]$, which means that the standard Galerkin method solves exactly an underdiffusive equation. If the mesh is not fine enough ($|P_\mathrm{e}| > 1$), then $k^\star$ becomes complex and it is not correct anymore to say that the standard Galerkin method solves an underdiffusive equation.

4.3 The Connection Between the Hyperbolic Theory and the Discrete Parabolic Model

We prove that (under the necessary assumptions) when we apply a standard Galerkin discretization to the linear parabolic convection-diffusion equation, the velocity of propagation is not infinite anymore at the discrete level. On the contrary, a finite velocity of propagation can be defined in the discrete equations. We conclude that the standard Galerkin formulation introduces an "artificial" relaxation time. The proof requires $k^\star$ to be rearranged as

$$k^\star = k - k\left(1 - \frac{2P_\mathrm{e}}{\ln(\frac{1+P_\mathrm{e}}{1-P_\mathrm{e}})}\right) < k. \tag{55}$$

If we compare the diffusive coefficient $k^\star$ with the coefficient that results from using Cattaneo's law (this may be found in (45)) we conclude that when we solve (47) using the standard Galerkin method we obtain the solution of a Cattaneo-type transport problem defined by the relaxation time

$$\tau_G = \frac{h}{a}\left(\frac{1}{2P_\mathrm{e}} - \frac{1}{\ln(\frac{1+P_\mathrm{e}}{1-P_\mathrm{e}})}\right). \tag{56}$$

As a result, a finite velocity of propagation can be defined in the discrete equation (49), namely

$$c_G = \frac{a}{(1 - 2P_\mathrm{e}/\ln(\frac{1+P_\mathrm{e}}{1-P_\mathrm{e}}))^{1/2}}. \tag{57}$$

Using relation (57) we can compute the value of "artificial" H (see (37) for a definition of H) introduced by the Galerkin method for a certain P_e. In Fig. 5 we plot the "artificial" H as a function of P_e. We conclude that when we solve problem (47) for $|P_\mathrm{e}| < 1$ using the standard Galerkin method we are actually solving a Cattaneo-type transport problem in subcritical flow conditions.

Remark 14 The Cattaneo-type problem that we actually solve when using the Galerkin formulation to discretize the linear parabolic model is defined by

$$a\frac{\mathrm{d}u}{\mathrm{d}x} - (k - \tau_G a^2)\frac{\mathrm{d}^2 u}{\mathrm{d}x^2} = 0; \quad x \in (0, L), \tag{58.1}$$

$$u(0) = u_0, \tag{58.2}$$

$$u(L) = u_L, \tag{58.3}$$

where τ_G is defined in (56). Problem (58) is a well-posed boundary-value problem for every value of the parameters k and τ_G. However, it only represents a Cattaneo-type convection-diffusion problem in subcritical flow. As we said before, (58.1) can be (under the assumption of sufficient regularity) used to describe the steady-state hyperbolic model, but boundary conditions have to be set in such a way that the one-dimensional counterpart of (28) is well-posed. Since

the one-dimensional counterpart of (28) is not well-posed subject to boundary conditions (58.2)–(58.3) in supercritical flow, problem (58) does not represent anymore a Cattaneo-type convection-diffusion problem in supercritical flow.

4.4 Stability Analysis of the Hyperbolic Model

Let us consider again the partition $\mathcal{P}$ that defines the mesh size h. We introduce the dimensionless number

$$H_{\mathrm{e}} = \frac{ah}{2(k - \tau a^2)} \tag{59}$$

which is the counterpart of P_{e} for the hyperbolic convection-diffusion theory [39, 40]. If we solve (58) by using the standard Galerkin method and linear finite elements (this is equivalent to second-order centered finite differences for this case), we find the following difference equations [38]:

$$(1 - H_{\mathrm{e}})u_{j+1} - 2u_j + (1 + H_{\mathrm{e}})u_{j-1} = 0;$$
$$\forall j = 1, \ldots, N - 1. \tag{60}$$

In the same way as (49), difference equations (60) can be solved exactly and the stability condition

$$|H_{\mathrm{e}}| \leq 1 \tag{61}$$

can be found. Relation (61) illustrates that in the hyperbolic model numerical instabilities do not arise for large values of the fluid velocity a, but for values of $|a|$ close to the pollutant velocity c. Indeed, the size of the velocities interval that leads to unstable solutions is

$$I = h/\tau. \tag{62}$$

We prove the above assertion by finding the a values that make

$$|H_{\mathrm{e}}| = 1 \tag{63}$$

which are given by

$$a_1 = -\frac{h}{4\tau} - \sqrt{\left(\frac{h}{4\tau}\right)^2 + c^2}, \tag{64.1}$$

$$a_2 = -\frac{h}{4\tau} + \sqrt{\left(\frac{h}{4\tau}\right)^2 + c^2}, \tag{64.2}$$

$$a_3 = -a_2, \tag{64.3}$$

$$a_4 = -a_1. \tag{64.4}$$

It is straightforward that $a_1 < 0$, $a_1 < -c$, $a_2 > 0$, $a_2 < c$. Taking into account all of this, the size of the velocities interval that makes the numerical solution unstable is given by

$$I = a_4 - a_2 + a_3 - a_1 = -2(a_1 + a_2) = h/\tau \tag{65}$$

which concludes the proof.

Remark 15 The size of the interval I decreases as τ increases which suggests that the numerical solution of the hyperbolic convection-diffusion theory becomes more stable as τ increases.

Remark 16 All the theoretical results presented in section 4 have been confirmed by numerical experiments in [41].

5 Finite Element Formulation of the Hyperbolic Convection-Diffusion Theory

The scientific literature on numerical methods for hyperbolic systems is vast [29, 36, 51, 65, 79, 83, 91]. Our numerical formulation for the hyperbolic convection-diffusion theory is based on the finite element method [53]. One of the most successful finite element formulations for hyperbolic problems is the Taylor-Galerkin method that was first proposed in [28] (see also [29–31]). Our numerical formulation is based on the Taylor-Galerkin method.

5.1 Continuous Problem in the Weak Form

We begin by considering a weak form of the hyperbolic convection-diffusion model. Let $\mathcal{V}$ and $\mathcal{W}$ denote the trial solution and weighting functions spaces, respectively. We assume that $U \in \mathcal{V}$ implies strong satisfaction of boundary conditions and $W \in \mathcal{W}$ entails homogeneity of the corresponding components of W. Therefore, the variational formulation is stated as follows: find $U \in \mathcal{V}$ such that $\forall W \in \mathcal{V}$,

$$B_C(W, U) = 0, \tag{66}$$

where

$$B_C(W, U) = \left(W, \frac{\partial U}{\partial t}\right)_\Omega - (\nabla W, F)_\Omega$$
$$+ (W, Fn)_\Gamma - (W, S)_\Omega. \tag{67}$$

In equation (67), $(\cdot, \cdot)_\Omega$ denotes the $\mathcal{L}^2$-inner product with respect to the domain Ω. The integration by parts of equation of (67), under the assumption of sufficient regularity, leads to the Euler-Lagrange form of (67)

$$\left(W, \frac{\partial U}{\partial t}\right)_\Omega + (W, \nabla \cdot F)_\Omega - (W, S)_\Omega = 0 \tag{68}$$

which implies the weak satisfaction of equation (28).

5.2 Time Integration

For the time integration we replace the time derivative in (67) by its second order Taylor expansion, namely

$$\frac{\partial \boldsymbol{U}}{\partial t}(\cdot, t^n) = \frac{\boldsymbol{U}(\cdot, t^{n+1}) - \boldsymbol{U}(\cdot, t^n)}{\Delta t}$$
$$- \frac{\Delta t}{2} \frac{\partial^2 \boldsymbol{U}}{\partial t^2}(\cdot, t^n) + \theta(\Delta t^2) \qquad (69)$$

where $\Delta t = t^{n+1} - t^n$ and $\theta(\Delta t^2)$ is an error of the order of Δt^2. Using the notation $\Delta t\, \Delta \boldsymbol{U}(\cdot) = \boldsymbol{U}(\cdot, t^{n+1}) - \boldsymbol{U}(\cdot, t^n)$ and rewriting the second-order time derivative in (69) in terms of spatial derivatives using the original equation (28), the following variational equation is found (the details may be found in [41]): find $\boldsymbol{U} \in \mathcal{V}$ such that $\forall \boldsymbol{W} \in \mathcal{V}$

$$B_{SD}(\boldsymbol{W}, \boldsymbol{U}) = 0 \qquad (70)$$

with

$$B_{SD}(\boldsymbol{W}, \boldsymbol{U})$$
$$= (\boldsymbol{W}, \Delta \boldsymbol{U})_\Omega - \left(\boldsymbol{W}, \Delta t\, \boldsymbol{B} \left(\boldsymbol{I} + \frac{\Delta t}{2} \boldsymbol{B} \right) \boldsymbol{U} \right)_\Omega$$
$$- \left(\frac{\partial \boldsymbol{W}}{\partial x_i}, \Delta t (\boldsymbol{I} + \Delta t \boldsymbol{B}) \boldsymbol{A}_i \boldsymbol{U} - \frac{\Delta t^2}{2} \boldsymbol{A}_i \boldsymbol{A}_j \frac{\partial \boldsymbol{U}}{\partial x_j} \right)_\Omega$$
$$+ \left(\boldsymbol{W}, \Delta t (\boldsymbol{I} + \Delta t \boldsymbol{B}) \boldsymbol{A}_i n_i \boldsymbol{U} - \frac{\Delta t^2}{2} n_i \boldsymbol{A}_i \boldsymbol{A}_j \frac{\partial \boldsymbol{U}}{\partial x_j} \right)_\Gamma$$
$$(71)$$

where the $\boldsymbol{A}_i$'s are the Jacobian matrices of the flux $\boldsymbol{F}$, the n_i's are the components of $\boldsymbol{n}$, and repeated indices indicate summation. Finally, $\boldsymbol{B}$ is the Jacobian matrix of the source term $\boldsymbol{S}$, that is,

$$\boldsymbol{B} = \frac{\partial \boldsymbol{S}}{\partial \boldsymbol{U}} = \begin{pmatrix} 0 & 0 & 0 & 0 \\ 0 & -1/\tau & 0 & 0 \\ 0 & 0 & -1/\tau & 0 \\ 0 & 0 & 0 & -1/\tau \end{pmatrix}. \qquad (72)$$

5.3 Space discretization

For the space discretization of (71) we make use of the Galerkin method. We approximate (70)–(71) by the following variational problem over the finite element spaces: find $\boldsymbol{U} \in \mathcal{V}^h$ such that $\forall \boldsymbol{W} \in \mathcal{W}^h$

$$B_{SD}(\boldsymbol{W}^h, \boldsymbol{U}^h) = 0. \qquad (73)$$

5.4 Numerical Examples

In this section we present some numerical examples to illustrate the main features of the hyperbolic convection-diffusion theory. For the sake of simplicity we limit ourselves to two-dimensional domains.
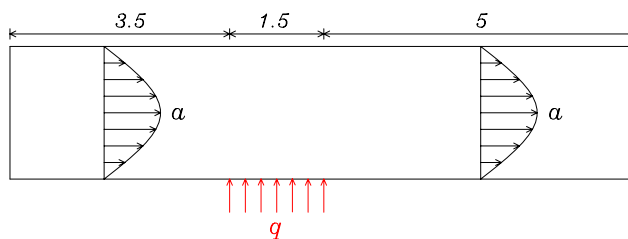
Fig. 6 Subcritical Poiseuille flow. Problem setup

### 5.4.1 Subcritical Poiseuille Flow

This example shows the evolution of a pollutant spillage between two parallel plates. Our computational domain is $\overline{\Omega} = [0, 10] \times [0, 2]$ (see Fig. 6). There is no pollutant in the domain at the initial time. The evolution of the pollutant is driven by a normal flux prescribed on the bottom boundary as indicated in Fig. 6. The prescribed normal flux takes the dimensionless value $\boldsymbol{q} \cdot \boldsymbol{n} = -2 \times 10^{-2}$. On the rest of the top and bottom boundaries we prescribe solid wall conditions. On the inflow boundary we impose vanishing concentration and tangential flux. On the outflow boundary we impose vanishing normal flux. The fluid velocity is given by a parabolic profile defined as $\boldsymbol{a}(x_1, x_2) = (x_2(2 - x_2), 0)^T$ and represented in Fig. 6. We select the physical parameters in such a way that the flow is subcritical everywhere and the maximum value of the H number is $H_{\max} = 1/\sqrt{2}$. The computational mesh is comprised of 50×10 bilinear elements. The time step size is $\Delta t = 0.02$. In Fig. 7 we represent (from top to bottom) the concentration solutions at dimensionless times $t = 0$, $t = 4.82$, $t = 9.62$, $t = 14.42$, $t = 19.22$ and the steady state solution. We observe that in subcritical flow the pollutant may propagate downstream and upstream.

5.5 Supercritical Poiseuille Flow

This example is the supercritical counterpart of the previous one. The computational domain and the velocity field are the same as in the previous example, but we changed the physical parameters to make the flow supercritical almost everywhere. The flow is defined by the maximum H number which in this case takes the value $H_{\max} = 10$. Given that the flow is supercritical, we need to prescribe all variables on the inflow boundary and none on the outflow boundary. The prescribed normal flux is on the bottom boundary is $\boldsymbol{q} \cdot \boldsymbol{n} = -10^{-2}$. The computational mesh is comprised of 70×10 bilinear elements. The time step size is $\Delta t = 0.02$.

In Fig. 8 we represent (from top to bottom) the concentration solutions at dimensionless times $t = 0$, $t = 3$, $t = 6$, $t = 9$, $t = 12$, $t = 15$ and the steady state solution. We observe that in supercritical flow the pollutant may not propagate upstream.

Fig. 7 Subcritical Poiseuille flow. We represent from top to bottom, concentration initial condition and solutions at dimensionless times $t = 4.82$, $t = 9.62$, $t = 14.42$, $t = 19.22$ and steady state
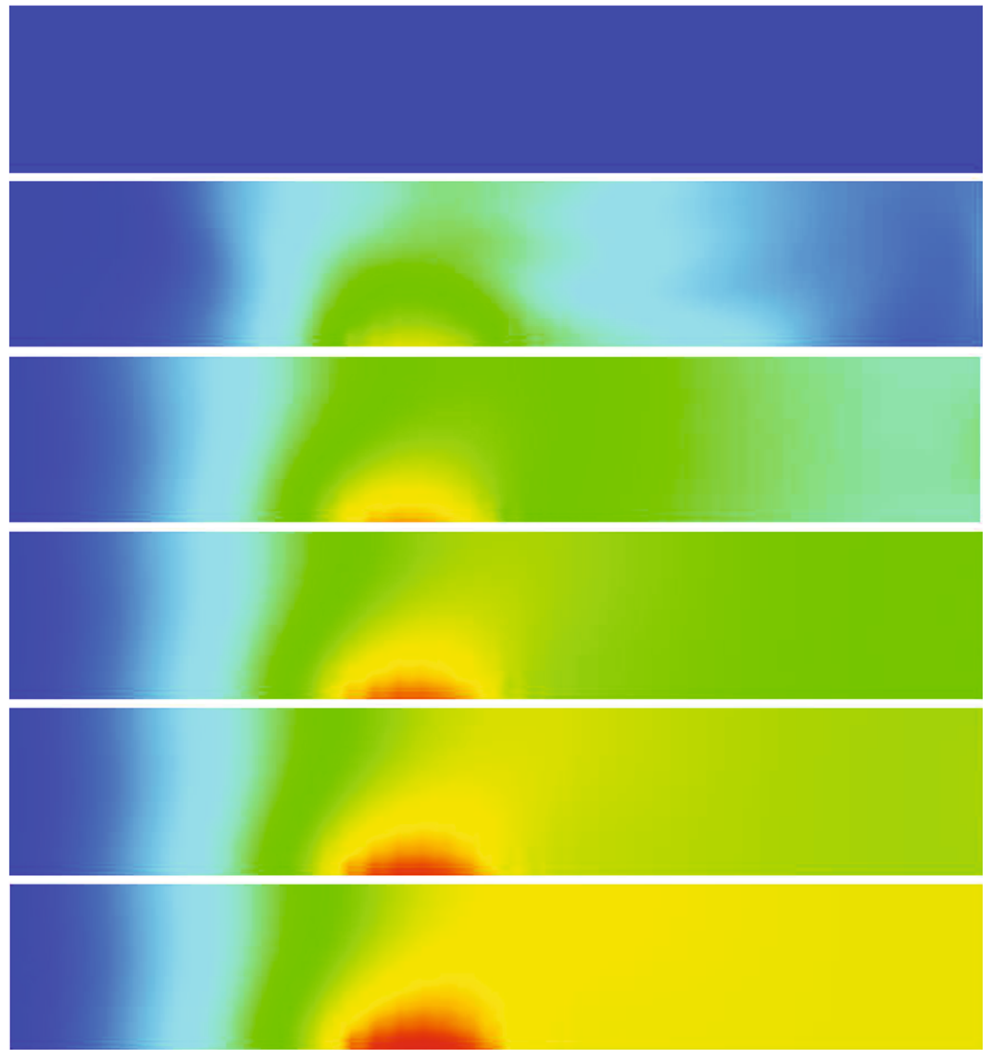
### 5.6 Practical Case in Environmental Engineering

In this section we simulate the evolution of an accidental spillage in the port of A Coruña (Spain). The domain of the problem comprises the whole area of the port. We represent the layout of the port in Fig. 9. To bound the domain of the problem we define an open-sea boundary from the end of Barrie's dike to the extreme of Oza's dock. The resulting computational domain has been depicted in Fig. 10 (left). As shown in this figure some elements of the real domain have been removed in order to simplify mesh generation. However, the omission of these elements is not important for the solution of the problem [34]. For instance, the oil tanker pier allows both water and pollutant to flow through it, so it does not modify the solution.

Three kinds of boundaries are differentiated in Fig. 10 (left): the solid wall boundary has been plotted as a green line; the boundary where the spillage takes place is plotted as a red line; the open-sea boundary is been plotted as a blue line.

The objective of this example is to show that the hyperbolic convection-diffusion theory has potential in representing mass transfer phenomena in engineering applications. For this reason we have not considered necessary to perform an accurate estimation of the parameters which would entail significant experimental work. A typical value for engineering calculations has been selected for the diffusivity k [52]. The estimation of the relaxation time τ is not so trivial since only the order of magnitude of the parameter can be estimated without making experiments. However, what really determines the solution is the ration between the fluid velocity a and the pollutant velocity $c = \sqrt{k/\tau}$. This quotient defines the dimensionless number introduced in (37).

In order to reduce the computations, the velocity field has not been calculated, but it was generated with two constraints: (a) it verifies the continuity equation for incompressible flow and (b) it satisfies standard boundary conditions for a viscous flow. We plot the velocity field in Fig. 10 (left). On the right hand side of Fig. 10 we have depicted the computational mesh.

Fig. 8 Supercritical Poiseuille flow. We represent from top to bottom, concentration initial conditions and solutions at dimensionless times $t = 3$, $t = 6$, $t = 9$, $t = 12$, $t = 15$ and steady state
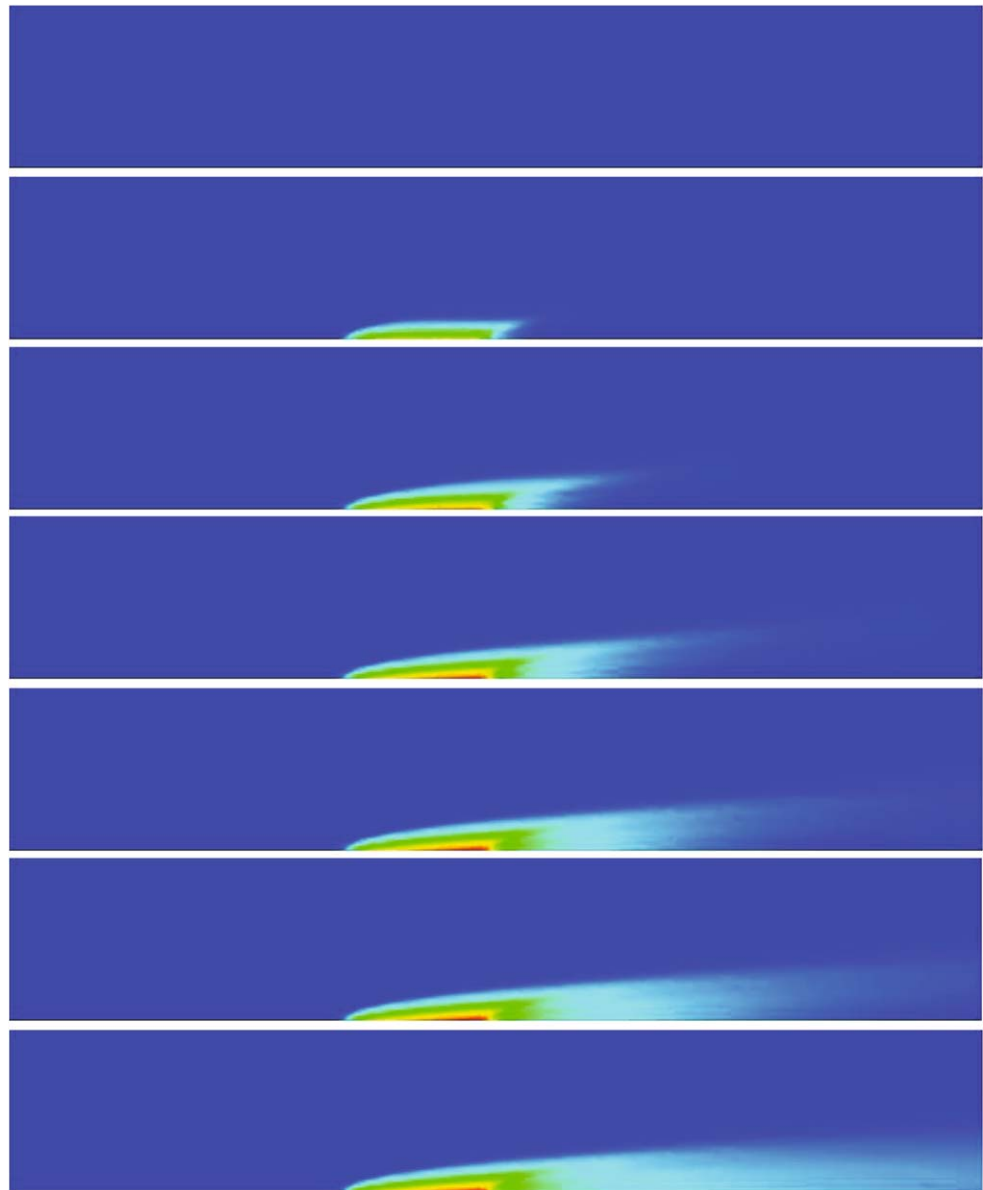
On the solid wall boundary we impose $\boldsymbol{q} \cdot \boldsymbol{n} = 0$. On the boundary where the spillage takes place we set the condition $\boldsymbol{q} \cdot \boldsymbol{n} = -10^{-2}$. On the open-sea boundary we impose $\boldsymbol{q} \cdot \boldsymbol{n} = cu$ where $c = \sqrt{k/\tau}$ is the pollutant wave velocity. The flow is given by H numbers (see (37)) verifying $H \leq H_{\max} \approx 0.3237$ what makes the flow subcritical everywhere. The computation was performed taking a maximum CFL number $C_{\max} \approx 0.5531$.

In Fig. 11 we show the initial concentration and concentration solutions at dimensionless times $t = 30$, $t = 60$ and $t = 90$. In Fig. 12 we plot concentration solutions at dimensionless times $t = 120$, $t = 150$, $t = 300$ and $t = 1000$.

Remark 17 This computation was repeated on finer meshes in space and time. Also, the calculations were repeated using

a Runge-Kutta discontinuous Galerkin method [43]. We did not find significant differences in any case.

6 Discontinuous Galerkin Formulation of the Hyperbolic Convection-Diffusion Theory

The numerical formulation presented in the previous section and the numerical examples previously analyzed illustrate the main characteristics of the hyperbolic convection-diffusion theory. However, the Galerkin formulation employed for the spatial discretization does not exhibit good stability properties when applied to hyperbolic partial-differential equations. We feel that the discontinuous Galerkin (DG) method represents a better choice for our hyperbolic

convection-diffusion theory. For this reason, we introduce a DG formulation.

The DG method is usually attributed to Reed and Hill [72]. Since its introduction in the framework of transport of neutrons in 1973, DG methods have evolved in a manner that made them suitable for computational fluid dynamics [18]. One of the most significant achievements using this method-
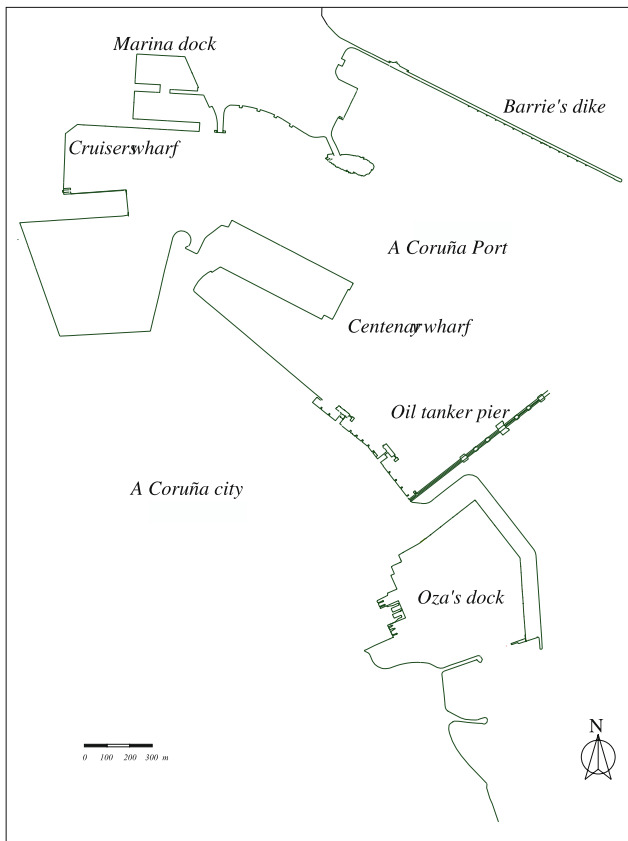

Fig. 9 Simulation of an accidental spillage in the port of A Coruña. Layout of the port

Fig. 10 (Color online) Simulation of an accidental spillage in the port of A Coruña. Velocity field and types of boundaries (*left*) and computational mesh of the problem (*right*). On the left hand side the solid wall boundary is been plotted as *a green line*; the boundary where the spillage takes place has been plotted as *a red line*; the open sea boundary is plotted as *a blue line*. The finite element mesh consists of 2023 bilinear elements and it was generated by using the code GEN4U [75]

ology is due to Cockburn and Shu who introduced the Runge-Kutta Discontinuous Galerkin Method [19–22].

Whereas the continuous finite element methods were initially developed for elliptic equations, the DG method was primarily applied to hyperbolic problems. However, there has been extensive research lately on DG methods for parabolic and elliptic equations [4, 8–10, 13, 14, 23]. Probably, the first successful study is due to Bassi and Rebay [8] who treated the viscous term in the Navier-Stokes equations within the DG framework. This method was followed by a paper by Cockburn and Shu [23] introducing the Local Discontinuous Galerkin method. To use any of these two methods it is necessary to split the second order Navier-Stokes (or convection-diffusion) equations in a system of first order equations. Then, a DG-type discretization is used for both resulting equations. However, the application of the DG method to our hyperbolic convection-diffusion theory is natural due to the wave-like structure of its solution. We define our DG method in the next section.

6.1 Space Discretization

The system to be solved is (28) with adequate initial and boundary conditions. Let E be the closure of an open subset of Ω with smooth boundary. We obtain the continuous problem in the weak form by multiplying by test functions and integration by parts:

$$
\left(\boldsymbol{W}, \frac{\partial \boldsymbol{U}}{\partial t} \right)_E - (\nabla \boldsymbol{W}, \boldsymbol{F})_E - (\boldsymbol{W}, \boldsymbol{S})_E
$$
$$
+ (\boldsymbol{W}, \boldsymbol{F}\boldsymbol{n})_{\partial E} = 0. \tag{74}
$$

To define the DG method, let us denote by Ω^h a partition of the computational domain Ω into a mesh of elements E. We call $\mathcal{P}^m(E)$ the space of polynomials of degree at most m. We define our discrete space as,

$$
\mathcal{W}^h = \left\{ \boldsymbol{W}^h \in (\mathcal{L}^2(E))^3 : \boldsymbol{W}^h|_E \in \mathcal{P}^m(E), \forall E \in \Omega^h \right\}. \tag{75}
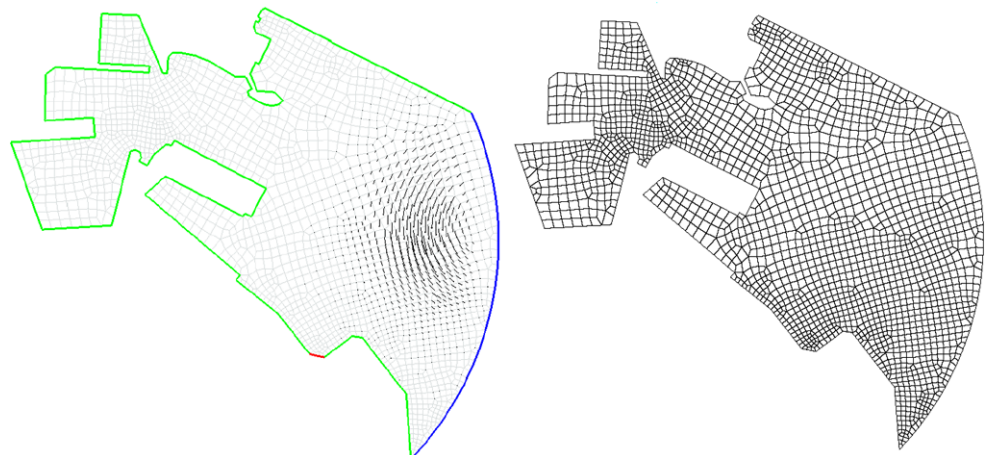$$

Fig. 11 Simulation of an
accidental spillage in the port of
A Coruña. We show (left to
right and top to bottom) the
concentration initial condition
and concentration solutions at
dimensionless times $t = 30$,
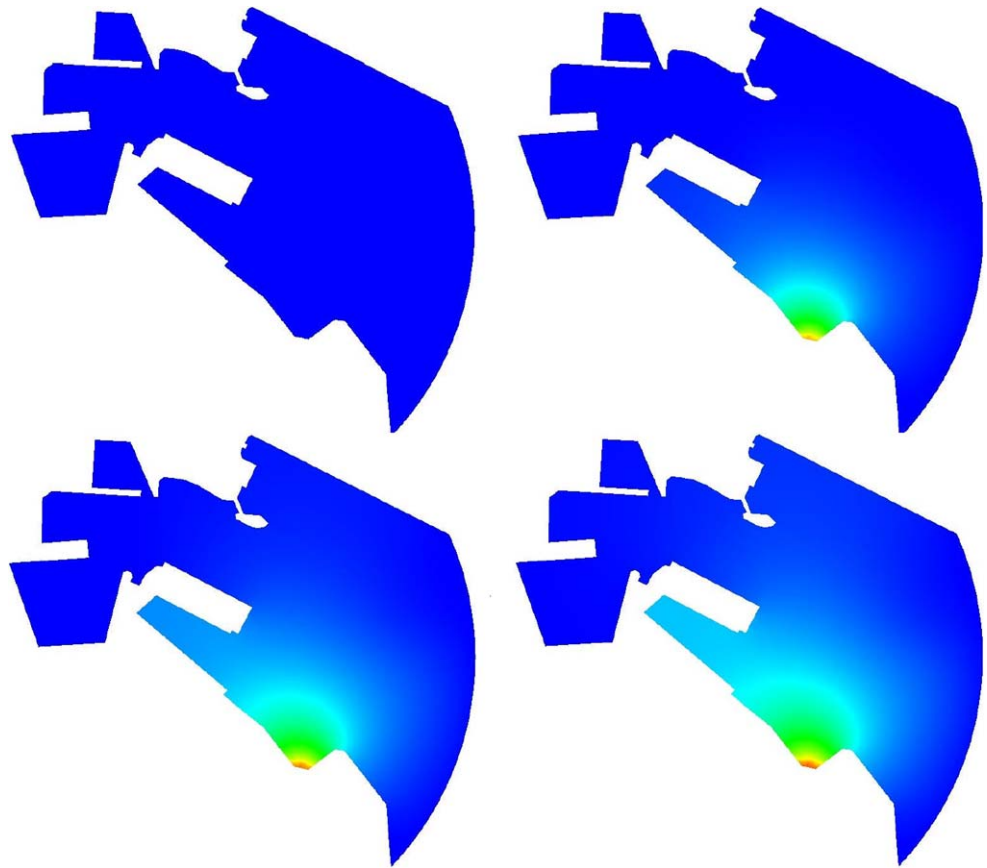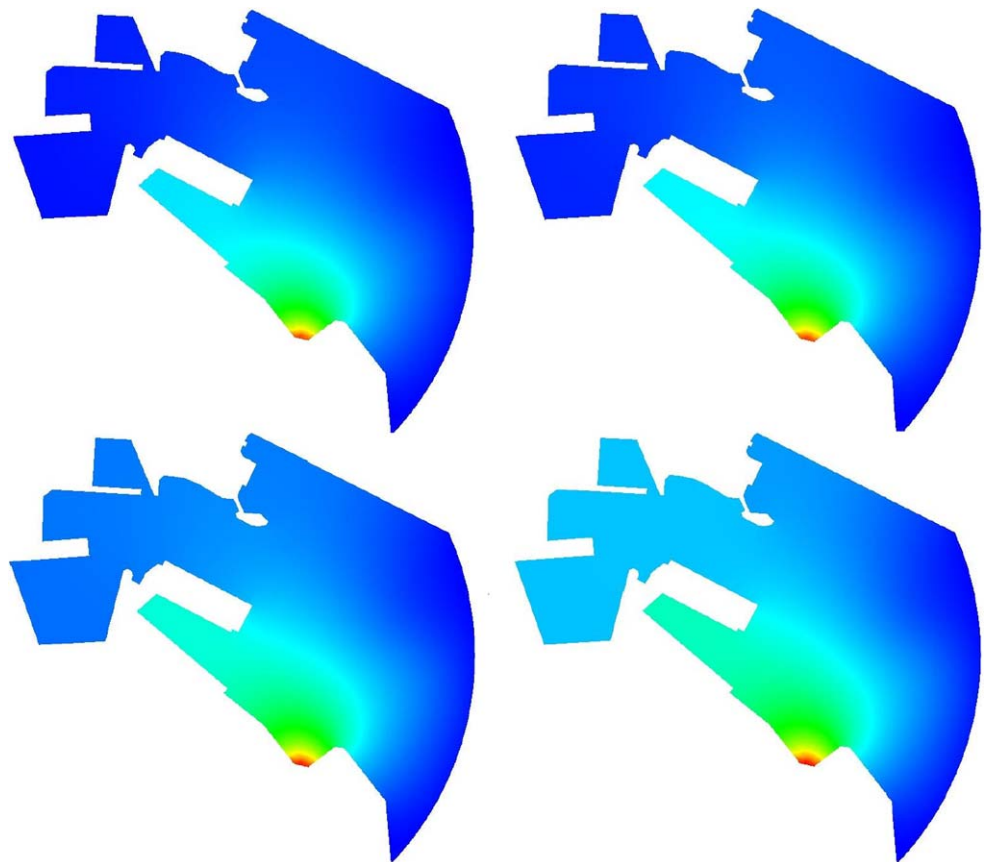$t = 60$ and $t = 90$

Fig. 12 Simulation of an
accidental spillage in the port of
A Coruña. We show (left to
right and top to bottom)
concentration solutions at
dimensionless times $t = 120$,
$t = 150$, $t = 300$ and $t = 1000$

Note that the discrete space does not enforce $\mathcal{C}^0$-continuity across the element boundaries. The variational problem over the finite-dimensional spaces is stated as: find $\boldsymbol{U}^h \in \mathcal{W}^h$ such that for all $E \in \Omega^h$.

$$B(\boldsymbol{W}^h, \boldsymbol{U}^h) = 0 \quad \forall \boldsymbol{W}^h \in \mathcal{W}^h \tag{76}$$

where

$$
\begin{aligned}
&B(\boldsymbol{W}^h, \boldsymbol{U}^h) \\
&= \left(\boldsymbol{W}^h, \frac{\partial \boldsymbol{U}^h}{\partial t} \right)_E - (\nabla \boldsymbol{W}^h, \boldsymbol{F}(\boldsymbol{U}^h))_E \\
&\quad - (\boldsymbol{W}^h, \boldsymbol{S}(\boldsymbol{U}^h))_E + \sum_{e \subset \partial E} (\boldsymbol{W}^h, \boldsymbol{H}^e(\boldsymbol{U}^h))_{\partial E}.
\end{aligned} \tag{77}
$$

In (77), $\boldsymbol{H}^e(\boldsymbol{U}^h)$ is an upwind numerical flux. To derive our numerical flux we follow the ideas of van Leer [80] and Hänel [49] who derived a numerical flux for the Euler equations (for an introduction to the concept of numerical flux the reader is referred to the books by Leveque [65] or Toro [79]). Let us suppose that e is the edge shared by elements E_1 and E_2 with $E_1 \equiv E$. Then, the numerical flux may be written as

$$\boldsymbol{H}^e(\boldsymbol{U}^h) = \boldsymbol{A}_+^e \boldsymbol{U}_1^e + \boldsymbol{A}_-^e \boldsymbol{U}_2^e \tag{78}$$

where $\boldsymbol{U}_i^e$ is the solution on the edge e as seen by the element E_i, $i = 1, 2$. Matrices $\boldsymbol{A}_+^e$ y $\boldsymbol{A}_-^e$ are defined by

$$\boldsymbol{A}_\pm^e \boldsymbol{C}_n^e = \boldsymbol{C}_n^e \boldsymbol{\Lambda}_{n\pm}^e \tag{79}$$

where

$$
\boldsymbol{\Lambda}_{n\pm}^e = \begin{pmatrix} \frac{\boldsymbol{a}\cdot\boldsymbol{n}\pm|\boldsymbol{a}\cdot\boldsymbol{n}|}{2} & 0 & 0 & 0 \\ 0 & \frac{\boldsymbol{a}\cdot\boldsymbol{n}\pm|\boldsymbol{a}\cdot\boldsymbol{n}|}{2} & 0 & 0 \\ 0 & 0 & \frac{\boldsymbol{a}\cdot\boldsymbol{n}-c\pm|\boldsymbol{a}\cdot\boldsymbol{n}-c|}{2} & 0 \\ 0 & 0 & 0 & \frac{\boldsymbol{a}\cdot\boldsymbol{n}+c\pm|\boldsymbol{a}\cdot\boldsymbol{n}+c|}{2} \end{pmatrix}
\tag{80}
$$

and $\boldsymbol{C}_n^e$ is the matrix defined in (35).

6.2 Time Discretization

Assembling together all the elemental contributions, the system of ordinary differential equations that governs the evolution of the discrete solution can be written as

$$M \frac{d\mathcal{U}}{dt} = \boldsymbol{R}(\mathcal{U}), \tag{81}$$

where M denotes the mass matrix, $\mathcal{U}$ is the global vector of degrees of freedom and $\boldsymbol{R}(\mathcal{U})$ is the residual vector. Due to the block diagonal structure of matrix M, the time integration of this system can be effectively accomplished using a explicit method for initial value problems. In this work we use the third-order TVD-Runge-Kutta method proposed by Shu and Osher [77]. Given the solution at the n-th step $\mathcal{U}^n$, the solution at the next time level $\mathcal{U}^{n+1}$ is computed in three steps as follows:

$$\mathcal{U}^{(1)} = \mathcal{U}^n + \Delta t \boldsymbol{L}(\mathcal{U}^n), \tag{82.1}$$

$$\mathcal{U}^{(2)} = \frac{3}{4}\mathcal{U}^n + \frac{1}{4}\mathcal{U}^{(1)} + \frac{1}{4}\Delta t \boldsymbol{L}(\mathcal{U}^{(1)}), \tag{82.2}$$

$$\mathcal{U}^{n+1} = \frac{1}{3}\mathcal{U}^n + \frac{2}{3}\mathcal{U}^{(2)} + \frac{2}{3}\Delta t \boldsymbol{L}(\mathcal{U}^{(2)}), \tag{82.3}$$

where $\boldsymbol{L}(\mathcal{U}) = M^{-1}\boldsymbol{R}(\mathcal{U})$. To compute $\boldsymbol{L}(\mathcal{U})$ at each time step we do not need to calculate M^{-1}. Instead of that, we compute the Cholesky factorization of the mass matrix at the first time step and we perform the necessary back and forward substitutions at each time iteration.

6.3 Numerical Examples

In this section we present some numerical examples to test out our DG formulation. We focus on the accuracy of the formulation for smooth solutions and its robustness for convection-dominated flows.

6.3.1 One-Dimensional Problems

This example shows that our DG formulation achieves optimal rates of convergence for concentration and flux when the solution is smooth. The model problem is the hyperbolic convection-diffusion equation defined on the domain $\overline{\Omega} = [0, 1]$. The parameters are $k = 1$, $\tau = 1$ and $a = 0.5$ which leads to subcritical flow. We consider the boundary conditions $u(0) = 0$, $u(1) = 1$ which are a legitimate choice in subcritical flow. We will use the presented DG method to compute the steady state solution. Then, we will compare the numerical solution with the exact solution of the steady problem to obtain the error. The time step is taken small enough so that the error can be assumed to arise from the spatial discretization. Within each element we interpolate the solution using polynomials of degree m. We present the results for $m = 1$ and $m = 2$. The optimal order of accuracy ($m + 1$) is achieved in both, concentration and pollutant flux as shown in Tables 2–5.

In some cases the optimal order of accuracy is not exactly achieved, but we believe that it is due to the roundoff errors and the tolerance in considering the solution steady.

6.3.2 Advection Skew to the Mesh

The problem setup is described in Fig. 13. The parameters are given by $k = 10^{-7}$, $\tau = 1$, $\boldsymbol{a} = (\cos(\alpha), \sin(\alpha))$. The computational domain is $\overline{\Omega} = [0, 1] \times [0, 1]$. Within this domain we define a computational mesh of 20×20 square

biquadratic elements. The flow is supercritical everywhere. Therefore, we must prescribe all the unknowns on the inflow boundary while no boundary conditions must be imposed on the outflow border. On the inflow boundary we

Table 2 $\| \cdot \|_\infty$ and $\| \cdot \|_2$ concentration errors and numerical order of accuracy. Linear elements. $k = 1$, $\tau = 1$, $a = 0.5$

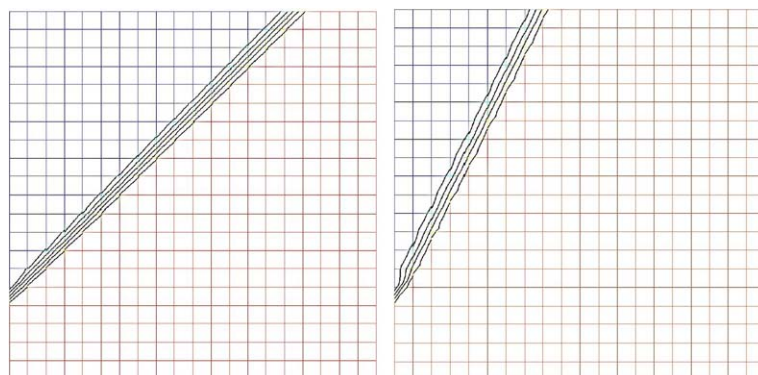| Elements	$\|\mathbf{Error}\|_\infty$	Order $\| \cdot \|_\infty$	$\|\mathbf{Error}\|_2$	Order $\| \cdot \|_2$
5	7.0149×10^{-3}	–	2.9403×10^{-3}	–
10	1.9811×10^{-3}	1.83	7.9018×10^{-4}	1.90
20	5.2591×10^{-4}	1.92	2.1538×10^{-4}	1.88
40	1.3885×10^{-4}	1.93	5.6566×10^{-5}	1.93
80	3.5664×10^{-5}	1.96	1.4493×10^{-5}	1.97

Table 3 $\| \cdot \|_\infty$ and $\| \cdot \|_2$ pollutant flux errors and numerical order of accuracy. Linear elements. $k = 1$, $\tau = 1$, $a = 0.5$

Elements	$\|\mathbf{Error}\|_\infty$	Order $\| \cdot \|_\infty$	$\|\mathbf{Error}\|_2$	Order $\| \cdot \|_2$
5	1.5607×10^{-2}	–	9.1734×10^{-3}	–
10	3.8745×10^{-3}	2.01	2.3406×10^{-3}	1.97
20	1.0109×10^{-3}	1.94	5.9517×10^{-4}	1.98
40	2.6091×10^{-4}	1.96	1.5010×10^{-4}	1.99
80	6.6288×10^{-5}	1.98	3.7693×10^{-5}	2.00

Table 4 $\| \cdot \|_\infty$ and $\| \cdot \|_2$ concentration errors and numerical order of accuracy. Quadratic elements. $k = 1$, $\tau = 1$, $a = 0.5$

Elements	$\|\mathbf{Error}\|_\infty$	Order $\| \cdot \|_\infty$	$\|\mathbf{Error}\|_2$	Order $\| \cdot \|_2$
5	1.2313×10^{-4}	–	6.5825×10^{-5}	–
10	1.5790×10^{-5}	2.96	8.6646×10^{-6}	2.93
20	2.0916×10^{-6}	2.92	1.1112×10^{-6}	2.96
40	2.6937×10^{-7}	2.96	1.4100×10^{-7}	2.98
80	3.4207×10^{-8}	2.98	1.7967×10^{-8}	2.98

enforce $q = 0$ and the discontinuous concentration profile depicted in Fig. 13. We plot the steady state solutions for $\alpha = \arctan(1) = 45°$ and $\alpha = \arctan(2) \approx 63.43°$ in Fig. 14. The internal layer is captured within two elements. We remark that using our theory for convection-diffusion there is no boundary layer at the outlet when convection dominates diffusion.

6.3.3 Rotating Flow

This is an accuracy test. Classical upwind procedures exhibit excessive crosswind diffusion on this problem (see for

Table 5 $\| \cdot \|_\infty$ and $\| \cdot \|_2$ pollutant flux errors and numerical order of accuracy. Quadratic elements. $k = 1$, $\tau = 1$, $a = 0.5$

Elements	$\|\mathbf{Error}\|_\infty$	Order $\| \cdot \|_\infty$	$\|\mathbf{Error}\|_2$	Order $\| \cdot \|_2$
5	1.4723×10^{-4}	–	5.0684×10^{-5}	–
10	1.8043×10^{-5}	3.03	5.7567×10^{-6}	3.14
20	2.3157×10^{-6}	2.97	6.3246×10^{-7}	3.19
40	2.9365×10^{-7}	2.98	7.2585×10^{-8}	3.13
80	3.7256×10^{-8}	2.98	8.5612×10^{-9}	3.08
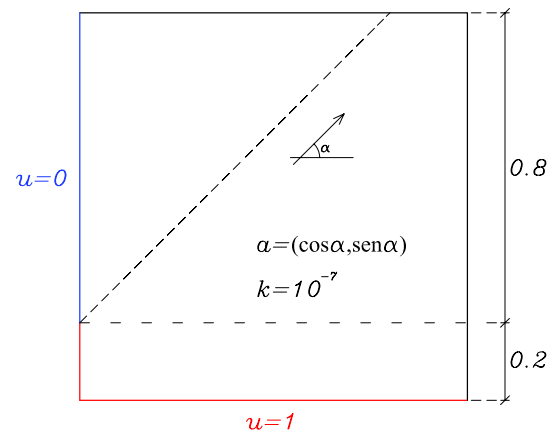
Fig. 13 Advection skew to the mesh. Problem setup. $k = 10^{-7}$, $\tau = 1$, $\boldsymbol{a} = (\cos \alpha, \sin \alpha)$

Fig. 14 Advection skew to the mesh. Steady state solution. $k = 10^{-7}$, $\tau = 1$, $\boldsymbol{a} = (\cos \alpha, \sin \alpha)$, $\alpha = \arctan(1)$ (*left*) and $\alpha = \arctan(2)$ (*right*)
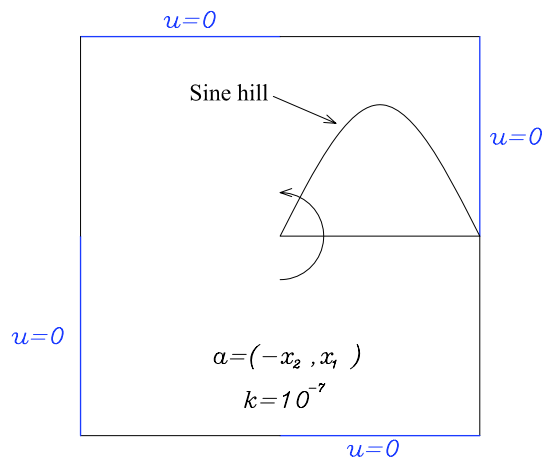
Fig. 15 Rotating flow. Problem setup. $k = 10^{-7}$, $\tau = 1$, $\boldsymbol{a} = (-x_2, x_1)$

Fig. 16 Rotating flow. Steady state solutions. $k = 10^{-7}$, $\tau = 1$, $\boldsymbol{a} = (-x_2, x_1)$

instance [11]). The problem setup is described in Fig. 15. The flow is circular about the center of the square domain $\overline{\Omega} = [-1, 1] \times [-1, 1]$ with a velocity field $\boldsymbol{a} = (-x_2, x_1)$. The parameters are given by $k = 10^{-7}$ and $\tau = 1$ which leads to supercritical flow everywhere except in a small circle centered in the origin of coordinates. We impose homogeneous boundary conditions (concentration and pollutant flux) on the inflow boundary whereas no boundary conditions are imposed on the outflow border. In addition, we enforce the condition $u(x_1, 0) = \sin(\pi x_1)$ on the slit $x_2 = 0$, $x_1 \in [0, 1]$. We use a uniform mesh comprised of 30×30 biquadratic elements. We plot the steady state solution in Fig. 16. The solution is very accurate and there is no appearance of crosswind diffusion.

7 Conclusions

Linear parabolic diffusion theories based on Fourier's or Fick's laws predict that disturbances can propagate at infinite speed. Although in some applications, the infinite speed paradox may be ignored, there are many other applications in which a theory that predicts propagation at finite speed is mandatory. As a consequence, several alternatives to the linear parabolic diffusion theory, with the objective of avoiding the infinite speed paradox, have been proposed over the years. This paper is devoted to the mathematical, physical and numerical analysis of a hyperbolic convection-diffusion theory. From our analysis and numerical results we conclude that our theory may have potential as a predictive tool in engineering analysis.

From the numerical point of view, we present two finite element formulations. The numerical examples illustrate the main characteristics of our model and the effectiveness and robustness of the numerical formulation. We also emphasize the differences of the parabolic and hyperbolic theories from the numerical point of view.
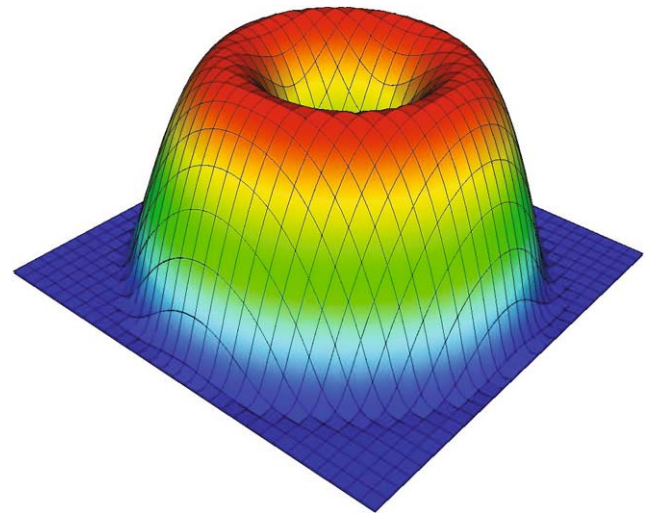
References

1. Ali YM, Zhang LC (2005) Relativistic heat conduction. Int J Heat Mass Transfer 48:2397–2406
2. Antontsev S, Díaz JI, Shmarev S (2002) Energy methods for free boundary problems. Applications to nonlinear PDEs and Fluid Mechanics, Series Progress in Nonlinear Differential Equations and Their Applications. Birkäuser, Basel
3. Arora M (1996) Explicit characteristic-based high resolution algorithms for hyperbolic conservation laws with stiff source terms. PhD dissertation, University of Michigan
4. Arnold DN, Brezzi F, Cockburn B, Marini D (2001) Unified analysis of discontinuous Galerkin methods for elliptic problems. SIAM J Numer Anal 39:1749–1779
5. Barenblatt GI (1952) On some unsteady motions of fluids and gases in a porous medium. Prikl Mat Mekh 16:67–78
6. Barenblatt GI (1996) Scaling, self-similarity, and intermediate asymptotics. Cambridge University Press, Cambridge
7. Barenblatt GI, Vishik MI (1956) On the finite speed of propagation in the problems of unsteady filtration of fluid and gas in a porous medium. Appl Math Mech (PMM) 34:655–662
8. Bassi F, Rebay S (1997) A high-order accurate discontinuous finite element method for the numerical solution of the compressible Navier-Stokes equations. J Comput Phys 131:267–279
9. Baumann CE, Oden JT (1999) A discontinuous hp finite element method for convection-diffusion problems. Comput Methods Appl Mech Eng 175:311–341
10. Baumann CE, Oden JT (1999) A discontinuous hp finite element method for the Euler and the Navier-Stokes equations. Int J Numer Methods Eng 31:79–95
11. Brooks A, Hughes TJR (1982) Streamline upwind/Petrov-Galerkin formulations for convection dominated flows with particular emphasis on the incompressible Navier-Stokes equations. Comput Methods Appl Mech Eng 32:199–259

12. Carey GF, Tsai M (1982) Hyperbolic heat transfer with reflection. Numer Heat Transfer 5:309–327

13. Castillo P (2002) Performance of discontinuous Galerkin methods for elliptic PDEs. SIAM J Sci Comput 24:524–547

14. Castillo P, Cockburn B, Perugia I, Schötzau D (2000) An a priori error analysis of the local discontinuous Galerkin method for elliptic problems. SIAM J Numer Anal 38:1676–1706

15. Cattaneo MC (1948) Sulla conduzione di calore. Atti Semin Mat Fis Univ Modena 3:3

16. Cattaneo MC (1958) Sur une forme de l'equation de la chaleur éliminant le paradoxe d'une propagation instantaneé. C R Acad Sci, Ser I Math 247:431–433

17. Christov CI, M Jordan P (2005) Heat conduction paradox involving second-sound propagation in moving media. Phys Rev Lett 94:4301–4304

18. Cockburn B, Karniadakis GE, Shu C-W (eds) (1999) Discontinuous Galerkin methods. Theory, computation and applications. Springer, Berlin

19. Cockburn B, Lin S-Y, Shu C-W (1989) TVB Runge-Kutta local projection discontinuous Galerkin finite element method for conservation laws III: one-dimensional systems. J Comput Phys 84:90–113

20. Cockburn B, Shu C-W (1989) TVB Runge-Kutta local projection discontinuous Galerkin finite element method for scalar conservation laws II: general framework. Math Comput 52:411–435

21. Cockburn B, Shu C-W (1998) The Runge-Kutta discontinuous Galerkin finite element method for conservation laws V: multidimensional systems. J Comput Phys 141:199–224

22. Cockburn B, Shu C-W (2001) Runge-Kutta discontinuous Galerkin methods for convection dominated flows. J Sci Comput 16:173–261

23. Cockburn B, Shu C-W (1998) The local discontinuous Galerkin method for time-dependent convection-diffusion systems. SIAM J Numer Anal 35:2440–2463

24. Codina R (1993) Stability analysis of the forward Euler scheme for the convection-diffusion equation using the SUPG formulation in space. Int J Numer Methods Eng 36:1445–1464

25. Compte A (1997) The generalized Cattaneo equation for the description of anomalous transport processes. J Phys A, Math Gen 30:7277–7289

26. Courant R, Hilbert D (1989) Methods of mathematical physics, vol II. Wiley, New York

27. Courant R, Friedrichs KO (1999) Supersonic flow and shock waves. Springer, Berlin

28. Donea J (1984) A Taylor-Galerkin method for convective transport problems. Int J Numer Methods Eng 20:101–120

29. Donea J, Huerta A (2003) Finite element methods for flow problems. Wiley, New York

30. Donea J, Quartapelle L, Selmin V (1987) An analysis of time discretization in the finite element solution of hyperbolic problems. J Comput Phys 70:463–499

31. Donea J, Quartapelle L (1992) An introduction to finite element methods for transient advection problems. Comput Methods Appl Mech Eng 95:169–203

32. Duhamel P (2004) Application of a new finite integral transform method to the wave model of conduction. Int J Heat Mass Transfer 47:573–588

33. Fick A (1855) Uber diffusion. Poggendorff's Ann Phys Chem 94:59–86

34. Figueroa CA, Colominas I, Mosqueira G, Navarrina F, Casteleiro M (1999) A stabilized finite element approach for advective-diffusive transport problems. In: Pimenta, PM, Brasil, R, Almeida, E (eds) Proceedings of the XX Iberian Latin-American congress on computational methods in engineering (CDROM), São Paulo, Brasil

35. Fourier JB (1822) Théorie analytique de la chaleur, Jacques Gabay

36. Godlewski E, Raviart P-A (1991) Numerical approximation of hyperbolic systems of conservation laws. Springer, Berlin

37. Goldstein S (1951) On diffusion by discontinuous movements and on the telegraph equation. Q J Mech Appl Math IV 2:2

38. Gomez H (2003) A new formulation for the advective-diffusive transport problem. Technical report, University of A Coruña (in Spanish)

39. Gomez H, Colominas I, Navarrina F, Casteleiro M (2004) An alternative formulation for the advective-diffusive transport problem. In: Mota Soares, CA, Batista, AL, Bugeda, G, Casteleiro, M, Goicolea, JM, Martins, JAC, Pina, CAB, Rodrigues, HC (eds) 7th congress on computational methods in engineering, Lisbon, Portugal

40. Gomez H, Colominas I, Navarrina F, Casteleiro M (2004) On the intrinsic instability of the advection–diffusion equation. In: Neittaanmäki, P, Rossi, T, Korotov, S, Oñate, E, Périaux, J, Knörzer, D (eds) Proc of the 4th European congress on computational methods in applied sciences and engineering (CDROM), Jyväskylä, Finland

41. Gomez H (2006) A hyperbolic formulation for convective-diffusive problems in CFD. PhD dissertation, University of A Coruña (in Spanish)

42. Gomez H, Colominas I, Navarrina F, Casteleiro M (2006) A finite element formulation for a convection-diffusion equation based on Cattaneo's law. Comput Methods Appl Mech Eng 196:1757–1766

43. Gomez H, Colominas I, Navarrina F, Casteleiro M (2007) A discontinuous Galerkin method for a hyperbolic model for convection-diffusion problems in CFD. Int J Numer Methods Eng 71:1342–1364

44. Gomez H, Colominas I, Navarrina F, Casteleiro M (2008) A mathematical model and a numerical model for hyperbolic mass transport in compressible flows. Heat Mass Transfer 45:219–226

45. Gurtin ME, Pipkin AC (1968) A general theory of heat conduction with finite wave speeds. Arch Ration Mech Anal 31:113

46. Grad H (1951) Principles of the kinetic theory of gases. In: Handbuch der Physik 12: Thermodynamics of gases. Springer, Berlin, p 205

47. Haji-Sheikh A, Minkowycz WJ, Sparrow EM (2002) Certain anomalies in the analysis of hyperbolic heat conduction. J Heat Transfer 124:307–319

48. Han-Taw C, Jae-Yuh L (1993) Numerical analysis for hyperbolic heat conduction. Int J Heat Mass Transfer 36:2891–2898

49. Hänel D, Schwane R, Seider G (1987) On the accuracy of upwind schemes for the resolution of the Navier-Stokes equations. AIAA Paper, 87-1005

50. Hoashi E, Yokomine T, Shimizu A, Kunugi T (2003) Numerical analysis of wave-type heat transfer propagating in a thin foil irradiated by short-pulsed laser. Int J Heat Mass Transfer 46:4083–4095

51. Hirsch C (2002) Numerical computation of internal and external flows, vol. II. Wiley, New York

52. Holley ER (1996) Diffusion and dispersion. In: Singh VP, Hager WH (eds) Environmental hydraulics. Kluwer Academic, Dordrecht, pp 111–151

53. Hughes TJR (2000) The finite element method. Linear static and dynamic finite element analysis. Dover, New York

54. Isaacson E, Keller HB (1966) Analysis of numerical methods. Wiley, New York

55. Jiang F, Sousa ACM (2005) Analytical solution for hyperbolic heat conduction in a hollow sphere. AIAA J Thermophys Heat Transfer 19:595–598

56. Jiang F (2006) Solution and analysis of hyperbolic heat propagation in hollow spherical objects. Heat Mass Transfer 42:1083–1091

57. Joseph DD, Preziosi L (1989) Heat waves. Rev Mod Phys 61:41–73

58. Joseph DD, Preziosi L (1990) Addendum to the paper "Heat waves". Rev Mod Phys 62:375–391

59. Jou D, Casas-Vázquez J, Lebon G (2001) Extended irreversible thermodynamics. Springer, Berlin

60. Kalashnikov AS (1987) Some problems of qualitative theory of non-linear second-order parabolic equations. Russ Math Surv 42:169–222

61. Kalatnikov IM (1965) Introduction to the theory of superfluidity. Benjamin, Elmsford

62. Kaliski S (1965) Wave equation for heat conduction. Bull Acad Pol Sci 4:211–219

63. Klages R, Radons G, Sokolov IM (2008) Anomalous transport: foundations and applications. Wiley, New York

64. Landau LD, Lifshitz EM (1959) Fluid mechanics. Pergamon, Elmsford

65. Leveque RJ (2002) Finite volume methods for hyperbolic problems. Cambridge University Press, Cambridge

66. Manzari MT, Manzari MT (1999) On numerical solution of hyperbolic heat equation. Commun Numer Methods Eng 15:853–866

67. Maxwell JC (1867) On the dynamical theory of gases. Philos Trans R Soc Lond 157:49–88

68. Oleynik OA, Kalashnikov AS, Yui-lin C (1958) The Cauchy problem and boundary problems for equations of the type of unsteady filtration. Izv USSR Acad Sci Ser Mat 22:667–704

69. Özisik MN, Tzou DY (1994) On the wave theory in heat conduction. ASME J Heat Transfer 116:526–535

70. Pattle RE (1959) Diffusion from an instantaneous point source with a concentration-dependent coefficient. Q J Mech Appl Math 12:407–409

71. Peshkov V (1944) Second sound in helium II. J Phys 8:381

72. Reed WH, Hill TR (1973) Triangular mesh methods for the neutron transport equation. Technical report LA-UR-73-479, Los Alamos Scientific Laboratory

73. Reverberi AP, Bagnerini P, Maga L, Bruzzone AG (2008) On the non-linear Maxwell-Cattaneo equation with non-constant diffusivity: Shock and discontinuity waves. Int J Heat Mass Transfer 51:5327–5332

74. Ruggeri T, Muracchini A, Seccia L (1990) Shock waves and second sound in a rigid heat conductor: a critical temperature for NaF and Bi. Phys Rev Lett 64:2640–2643

75. Sarrate J, Huerta A (2000) Efficient unstructured quadrilateral mesh generation. Int J Numer Methods Eng 49:1327–1350

76. Sharma KR (2008) On the solution of damped wave conduction and relaxation equation in a semi-infinite medium subject to constant wall flux. Int J Heat Mass Transfer 51:6024–6031

77. Shu C-W, Osher S (1988) Efficient implementation of essentially non-oscillatory shock-capturing schemes. J Comput Phys 77:439–471

78. Tavernier J (1962) Sue l'equation de conduction de la chaleur. C R Acad Sci 254:69

79. Toro EF (1999) Riemann solvers and numerical methods for fluid dynamics: A practical introduction. Springer, Berlin

80. Van Leer B (1982) Flux vector splitting for the Euler equations. Lect Notes Phys 170:507–512

81. Vázquez JL (2006) The porous medium equation. Mathematical theory. Oxford University Press, Oxford

82. Vick B, Özisik MN (1983) Growth and decay of a thermal pulse predicted by the hyperbolic heat conduction equation. ASME J Heat Transfer 105:902–907

83. Wesseling P (2001) Principles of computational fluid dynamics. Springer, Berlin

84. Whitham GB (1999) Linear and nonlinear waves. Wiley, New York

85. Wilhelm HE, Choi SH (1975) Nonlinear hyperbolic theory of thermal waves in metals. J Chem Phys 63:2119

86. Wu W, Li X (2006) Application of the time discontinuous Galerkin finite element method to heat wave simulation. Int J Heat Mass Transfer 49:1679–1684

87. Yabe T, Ishikawa T, Wang PY, Aoki T, Kadota Y, Ikeda F (1991) A universal solver for hyperbolic equations by cubic-polynomial interpolation II. Two- and three-dimensional solvers. Comput Phys Commun 66:223–242

88. Yang HQ (1992) Solution of two-dimensional hyperbolic heat conduction by high resolution numerical methods. AIAA-922937

89. Zakari M, Jou D (1993) Equations of state and transport equations in viscous cosmological models. Phys Rev D 48:1597–1601

90. Zel'dovich YB, Kompaneets AS (1950) On the theory of propagation of heat with thermal conductivity depending on temperature. In: Collection of papers dedicated to 70th birthday of AF Ioffe 61–71

91. Zienkiewicz OC, Taylor RL (2000) The finite element method, vol 3. Fluid dynamics. Butterworth Heinemann, Stoneham